Composite Structures 266 (2021) 113828

Contents lists available at ScienceDirect

Composite Structures

journal homepage: www.elsevier.com/locate/compstruct

Review

Friction-based processes for hybrid multi-material joining

Francesco Lambiase [a,*], Frank Balle [b], Lucian-Attila Blaga [c], Fengchao Liu [d], Sergio T. Amancio-Filho [e]

[a] Dept. of Industrial and Information Engineering and Economics, University of L'Aquila, via G. Gronchi 18, Zona Industriale di Pile, 67100 (AQ), Italy
[b] Department of Sustainable Systems Engineering (INATECH), Walter-and-Ingeborg-Herrmann-Chair for Power Ultrasonics and Engineering of Functional Materials, Faculty of Engineering, University of Freiburg, 79110 Freiburg, Germany
[c] Institute of Materials Research, Materials Mechanics, Department of Solid State Joining Processes, Helmholtz-Zentrum Geesthacht, Geesthacht, Germany
[d] Department of Naval Architecture and Marine Engineering, University of Michigan, Ann Arbor, MI 48109, USA
[e] Graz University of Technology—TU Graz, Institute of Materials Science, Joining and Forming, BMK Endowed Professorship for Aviation, Kopernikusgasse 24/1, 8010 Graz, Austria

ARTICLE INFO

Keywords:
Friction
Dissimilar materials
Multi-material-design
Welding
Lightweighting

ABSTRACT

The adoption of multi-material lightweight structures has been recognized as one of the most effective and promising solutions to improve fuel efficiency and accelerate the electrification of future transportation systems. A wider application of multi-material lightweight structures has been limited by our capability to fabricate them reliably and cost-effectively at a commercial scale. In the last decade, many friction-based joining processes have been developed and demonstrated their advantages over mechanical fastening and adhesive bonding processes in fabricating future multi-material lightweight structures. This article provides a comprehensive review on the recent advances of five promising friction-based joining processes (friction assisted joining, friction lap welding, friction spot joining, friction riveting, and ultrasonic welding) on the aspects of facilities, joining process, joining mechanism, applicable materials, surface pretreatments, and the influence of process parameters on the performance of the produce joints. This article also provides a summary of the performance of the produced joints under static load, dynamic load, various thermal cycles, or harsh chemical environments. The main similarities and differences among the joining processes are discussed. The paper points out the main knowledge gaps that need to be filled and the research that needs to be conducted to further advance the joining process. This review article will place the friction-based joining process at a new starting point with accelerated developing speed towards higher technical maturity to make the processes available for certifiable industrial applications.

Contents

1. Introduction . . . 2
2. Friction based joining processes . . . 3
   2.1. Friction-assisted joining . . . 3
   2.2. friction lap welding . . . 3
   2.3. Friction Riveting . . . 6
   2.4. Friction Spot Joining . . . 7
   2.5. Ultrasonic welding . . . 9
3. Friction-based process characteristics . . . 11
   3.1. Advantages of the friction-based welding process . . . 11
   3.2. Main process differences . . . 11
   3.3. Process design and control . . . 12
   3.4. Surface pre-treatments . . . 12
4. Discussion . . . 13
5. Conclusions . . . 15
   Declaration of Competing Interest . . . 16

* Corresponding author at: Monteluco di Roio, 67040 (AQ), Italy.
E-mail address: francesco.lambiase@univaq.it (F. Lambiase).

https://doi.org/10.1016/j.compstruct.2021.113828
Received 14 January 2021; Revised 26 February 2021; Accepted 6 March 2021
Available online 16 March 2021

Acknowledgments. 16
References 16

1. Introduction

The increasing demand for performance improvement, the pursuit of product customization, and the development of high-performance new materials are pushing towards a growing spread of multi-material components in civil, transport, aerospace, biomedical, etc. The weight reduction with uncompromised overall performance represents the most effective approach for the reduction of CO2 emissions, energy savings (e.g. in transport), and an increase in fuel economy. This is, for example, a crucial aspect for new generation electric vehicles as a reduction in vehicle weight (e.g. in chassis or components) can be exploited for the increase of the weight destined to the battery fleet and the consequent increase of fuel autonomy, which still represents one of the main limits in the diffusion of these vehicles.

The use of lightweight materials and an effective combination of different materials will enable considerable benefits with the intent to reduce the overall weight. The diffusion of light alloys and carbon fiber reinforced polymers (CFRP) in the automotive sector for D-segment vehicles and beyond requires the implementation of specific coupling processes. In recent years, increasing parts of the chassis in supercars, such as Ferrari, Lamborghini, and Mclaren are made of CFRP and are coupled with high strength steels or aluminum parts. More recently, the use of hybrid chassis (hybrid metal-composite chassis) has been extended to less expensive vehicles, such as the Alfa Romeo 4C, BMW 7-series, GMC Sierra CarbonPro, and Chevrolet Corvette Z06. Hybrid structures are also widely used in the civil sector, for example, CFRP components have been used as reinforcements in bridges [1] to increase the bending stiffness of aluminum beams [2], to repair and reinforce structural components [3–5], and even to protect from fire and thermal insulation of light-weight structural materials [6].

The coupling of dissimilar materials is often hampered by their difference in chemical composition, mechanical properties, and physical characteristics. The current established joining processes (mainly adhesive bonding and mechanical fastening) involve considerable limitations and disadvantages in the construction of multi-material components. Adhesive bonding is performed by using an interlayer between the two adherends. This process enables the formation of continuous joints, thus reduced stress concentration (around spot connections). However, adhesive bonding requires extensive pretreatments to remove superficial oil, grease, powder, and even surface oxide. This is typically performed through etching, grinding, and degreasing (these operations require solvents and other machining processes that lead to high environmental impact). To achieve a good load-bearing capability to shear stress while limited peeling strength, the component's edges are often machined and/or plastically deformed to avoid out-of-plane stress acting on the adhesive bonds. During the application of the adhesive as well as the entire curing phase a fine control of the adhesive distribution and the processing pressure is required since the adhesive thickness has a great influence on the mechanical behavior of the bond. Adhesive bonding requires special equipment, such as templates and jigs, to be specifically designed to fasten the components during the curing time. Finally, from a mechanical point of view, adhesive bonding suffers from long-time uncertainty and severe environmental sensitivity.

Traditional Mechanical Fastening (MF) processes also have their advantages and limitations. Except for few processes (such as hemming), MF generally involves spot connections that come with severe stress concentration around the connection. Besides, especially when fiber-reinforced polymers (FRP) are involved, the through-holes produced on the components for the insertion of the joining element cause fiber interruption. This may lead to a severe worsening of the mechanical strength of the joints. Also, external elements come with components overweighting and an increase in cost. From a process point of view, the drilling process increases the overall joining time. For this reason, some studies investigated alternative processes such as punching for the production of holes in the composite materials [7] or direct joining without hole drilling [8]. Nevertheless, mechanical fastening is still broadly used in many industrial fields because of the relatively high mechanical performances of the joints, higher joint reliability than adhesive, and the lack of mature joining solutions.

Recently, several joining processes have been developed to overcome the limitations of hybrid structure fabrication mentioned above. Thermomechanical joining processes represents a suitable alternative for the production of multi-material structures especially metal-polymer and metal-composite structures. Direct Laser joining of metal-polymer [9–15], ultrasonic welding [16–24] and joining [25–28], friction spot joining [29–35], friction lap welding [36–40], friction stir lap welding [41–43], friction stir welding [44], injection molding [45,46] and friction riveting [47–49] represent some of the examples. During thermomechanical joining processes, the components are heated using different means (e.g. laser source, friction, or ultrasonic displacement), and external pressure is applied to achieve the joint formation. This enables the development of different joining mechanisms e.g. Van der Waals, chemical bonds [50] as well as mechanical micro interlock [51], which often result in joints with high mechanical properties. During the joining process, the metal-polymer interface is heated up until a targeted temperature range (close to the softening/melting temperature of the polymer) is reached. Joining at temperatures below the targeted heating range lead to insufficient energy for the joining activation. On the other hand, the temperature at the metal-polymer interface is also limited by adverse overheating phenomena, including bubble formation, excessive thermal shrinkage, and even thermal degradation of the polymer. This may affect significantly the mechanical and chemical resistance of the joints. Also, join-

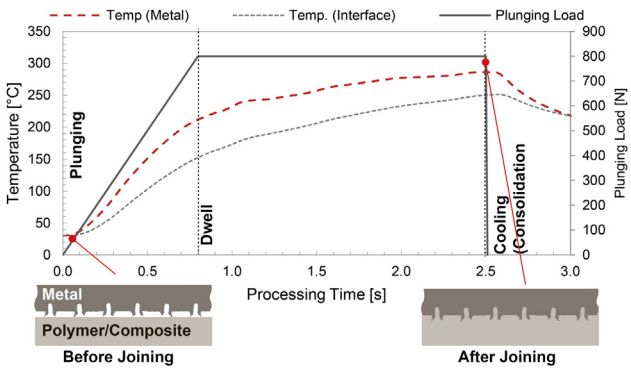

Fig 1. Force and temperature variation during the main phases of the friction-assisted Joining process.

ing at temperatures higher than needed also causes energy waste and prolonged processing time.

To accelerate the adoption of multi-materials lightweight structures through advancing the relevant manufacturing technologies, the present paper aimed at collecting and organizing the main results achieved by available research studies concerning hybrid metal-polymer and metal-composite joining processes. This was done with special attention to the required equipment, achieved mechanical strength as well as main defects produced during the joining operations. The paper firstly describes and benchmarks the main thermomechanical joining processes. Finally, a brief discussion on pre-treatments and possible improvements is reported.

2. Friction based joining processes

This section is subdivided into different subsections each of which summarized the main characteristics of each process.

- Friction-Assisted Joining
- Friction Lap Welding
- Friction Riveting
- Friction Spot Joining
- Ultrasonic Welding

2.1. Friction-assisted joining

Friction Assisted Joining (FAJ) is a joining-by-forming process particularly suited for the production of hybrid structures made of dissimilar materials. FAJ enables lap joints among metals, thermoplastics, and composite laminates. FAJ is based on mechanical interlocking resulting from the penetration of natural or artificial asperities on the metal bottom surface into the underlying component made of a softer material (a softer metal, a thermoplastic, or a fiber-reinforced thermoplastic). To increase the strength of the joints, the surface of the metal sheet is often pre-treated through laser micro-milling, machining, etc. This promotes the formation of enhanced interlocks and/or chemical bonds, leading to higher joint strength.

During the process, a rotating tool is plunged against the upper surface of the metal sheet. The tool is generally made of high-strength steels (for relatively soft metals) or tungsten carbide (for higher-strength materials, such as structural steels and titanium alloys) [52]. The friction produces frictional heat that is rapidly transferred to the joint interface owing to the great thermal conductivity of the metal component. As a result, the top of the bottom component is rapidly heated and softens. This enables the asperities at the bottom of the upper component to penetrate the softened material, forming mechanical interlocks. The process is subdivided into three phases, namely plunging, dwell, and cooling (tool retraction) [53], as schematized in Fig. 1. During the plunging phase, the tool, which rotates at a prescribed rotation speed (typically ranging between 4000–8000 RPM), is plunged against the upper component. This phase is preferably performed under load control and a constant plunge rate (100–1000 N/s). Then, as the targeted plunging load (reference values are 0.3–2 kN) is reached, the dwell phase begins. During this phase, the load acting on the tool is kept constant until the end of the dwell phase. The duration of the dwell phase should be selected to reach the desired temperature at the metal-polymer interface (typically close to the softening/melting temperature of the polymer, or polymeric matrix). In the end, the tool is rapidly retracted, enabling joint consolidation by cooling. The process is characterized by relatively low energy input (typically lower than 2 kJ [54]) and requires few seconds (even 1 s), to reach the targeted processing temperature. However, even though the process could be further shortened, this would produce steeper temperature gradients owing to localized heating that would affect the strength of the welds [55]. Besides, the adoption of a rotating element to produce frictional heat also leads to intrinsic temperature gradients as the relative velocity (and consequently the frictional heat) increases from the center to the edge of the tool pin.

The selection of the main process parameters is performed to achieve a certain softening of the lower sheet material. Thus, the selection of the tool rotation speed, plunging force, and dwell time, is mainly temperature driven. Unsuccessful joining conditions are generally due to:

- Formation of “cold joints”: the temperature at the interface is relatively low and does not enable enough sinking of the asperities on the upper surface in the underlying components;
- Excessively high temperatures: these conditions involve several adverse phenomena including, excessive thinning of the polymer, material reflow towards side directions, and polymer degradation;
- Formation of porosities: these are generally produced on hygroscopic materials whose moisture content gives rise to the formation of the bubbles when the temperature exceeds certain values;
- Pinhole: when excessively high pressure (owing to the adoption of high plunging loads and relatively small pin) is involved. This causes a heavy plunging of the upper sheet that leads to excessive thinning of both the components in the correspondence of the tool pin. This also involves adverse issues. When proper pressure is exerted on the upper sheet, thinning is generally limited to 0.05–0.1 mm.
- Severe modification of the polymer at the interface with the metal component: this is particularly significant when semi-crystalline polymers are involved. Here, the process-induced thermal cycles may significantly alter the crystallinity of the polymer inducing a severe reduction of the mechanical behavior [56].

As above-mentioned, the process is relatively simple and can be successfully performed employing low-power machines. In preliminary studies conducted by Lambiase *et al.* [52–55], simple equipment consisting of an instrumented drilling CNC machine was adapted to produce Friction Assisted Joining. The machine was equipped with axial load and torque sensors as shown in Fig. 2. Also, temperature measurements were performed using IR thermography. Thus, the main joining mechanism, a suitable processing window, and equipment requirements were determined. The machine involved a low-power motor (500 W) and relatively low torque (2 Nm). This limited the dimension of the tool pin diameter and consequently involved some issues (high pressure leading to the pinhole defect), low friction rate, etc.

Further developments of the FAJ process have been performed to verify the applicability of the process for joining metals and composite laminates with a thermoplastic matrix. Fig. 2 displays a cross-section of a specimen made by AA7075 alloy and CFRP with a Polyphenylene sulfide (PPS) matrix [57]. When woven laminates are used instead of pure thermoplastics, the material flow that triggers the formation of the mechanical interlocks is different. Here, the pressure exerted by the metal teeth on the underlying component involves a much smaller amount of material flow towards the grooves of the texture as the great stiffness and flow resistance imposed by the fiber’s structures (see Fig. 3).

2.2. friction lap welding

Friction lap welding (or friction lap joining) is a new joining method that can directly join metal and polymer together [58,59]. The process of friction lap welding is schematically illustrated in Fig. 4. A non-consumable cylindrical tool is set to rotate at a desirable speed (Fig. 4a) and then moved to press against the metal sheet placed above the thermoplastic sheet (Fig. 4b). Once the desired pressure and temperature are attained, the cylindrical tool is set to travel along the welding direction (Fig. 4c). The primary function of the cylindrical

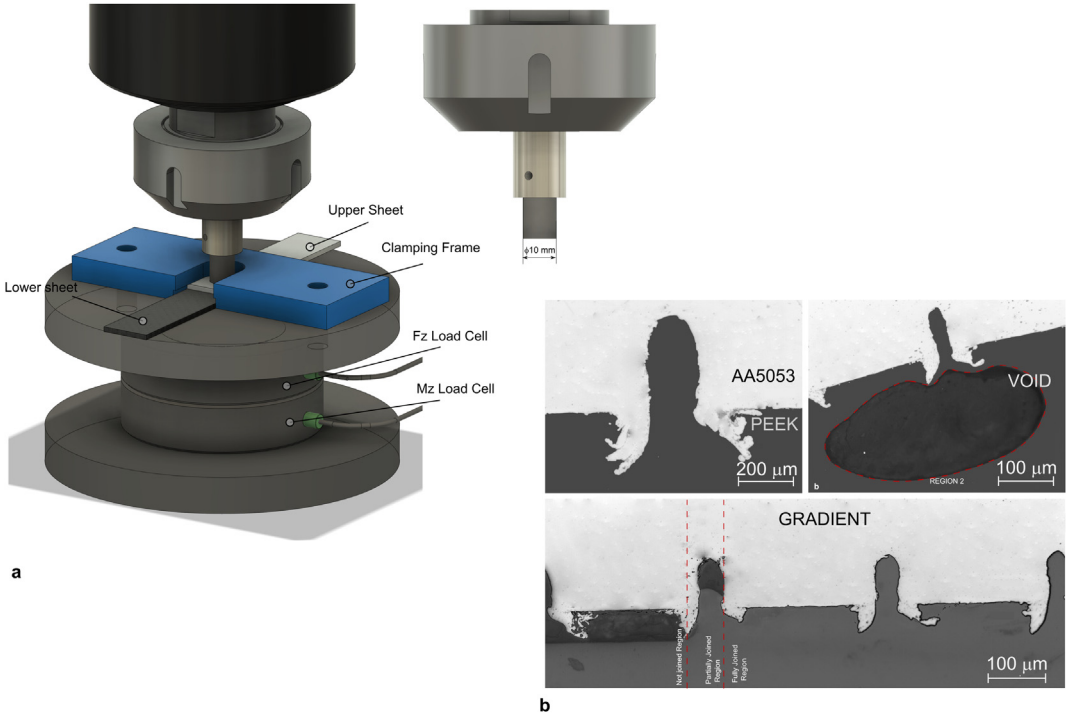

Fig 2. (a) Schematic of the experimental equipment used for FAJ and (b) characteristic regions of metal-polymer interface including optimal joining conditions, the formation of sub-superficial voids due to moisture content, and temperature gradient. (Reproduced with authorization from [55]).

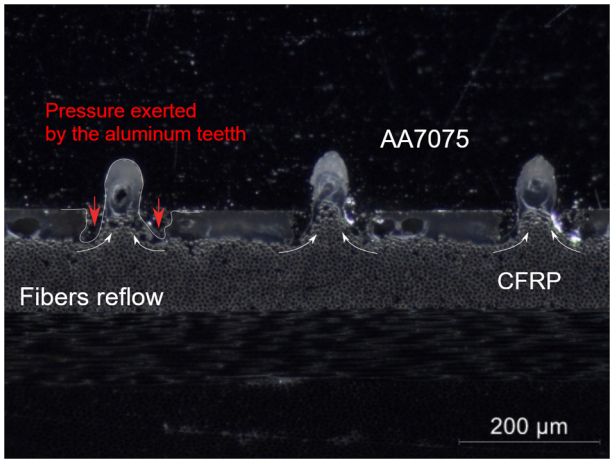

Fig 3. Material flow in aluminum-to-CFRP joint produced by friction assisted joining [57].

tool is to generate local frictional heat while exerting sufficient local pressure to form a joint between the plastic and metal pieces. A strong bond at the interface between the metal and polymer beyond mechanical interlocking has been proven recently by Liu et al. [50] through X-ray photoelectron spectroscopy (XPS) measurements. The available investigation has demonstrated that strong dissimilar joints of metal and polymer can be produced by friction lap welding over a wide range of parameters [58,60,61], including a high welding speed of 5 m/min [59]. Friction lap welding has been approved to be applicable for the combination of various metal and polymer components. The metal components include Al alloy [58,61], Mg alloy [59,60], coper [62] and steels [63] while the polymer components include polyamide (PA) [58,60,63], polyethylene (PE) [59], polypropylene (PP) [64] and carbon-fiber reinforced polymer (CFRP) [61,65].

If the thermoplastic polymer or the matrix of thermoplastic composites contain carbonyl groups (C═O), strong C—O—M bonds (where M represents a metal atom) can develop at the joint interface after friction lap welding, and therefore considerable joining strength can be achieved [50]. Fig. 5 shows a typical fracture surface of a lap shear test sample of the lap joints of PA and 6061Al produced by friction lap welding at a tool rotation rate of 3000 RPM and a welding speed of 1500 mm/min. The optical image (Fig. 5a) showed that a layer of PA film was left on the 6061 Al surface after the lap shear test. Scanning electron microscope (SEM) observation provides more details about the residual PA on the 6061 Al surfaces. Fractured detrital PA with tearing features was scattered on the Al surface. Ridge-shaped residual nylons which can cab be treated as crack propagation paths were also detectable. The occurrence of cohesive fracture can be ascribed to the formation of strong C—O—Al chemical bonds at the joint interface of PA and the Al alloy [58,50].

It is difficult to achieve chemical bonding between metal and polymers that do not contain carbonyl groups and therefore suitable surface modification is necessary before the joining [50]. For example, Liu *et al.* [59] have shown that magnesium alloy and polyethylene could not be directly joined without surface treatment. By treating the surface of the polyethylene with a corona discharge and the surface of a magnesium alloy with plasma electrolytic oxidation, Liu et al. successfully produced strong bonding between the materials through forming chemical bonds and micro mechanical interlocking. Similarity, Meyers *et al.* [64] produced strong lap joints of aluminum alloy and polyethylene using friction lap welding after pretreating aluminum alloy surface with laser.

The local friction heat during friction lap welding is affected by the size of the friction tool, applied to forge force (F), tool rotation rate (R), and tool traverse speed (v). An increase in tool size, forging force, and rotation rate will increase the heat input and welding temperature while an increase in traverse speed will reduce the local heat input. Higher local heat input will increase the thickness of melted thermoplastic polymer (H) under the metal sheet. Liu *et al.* [60] have demon-

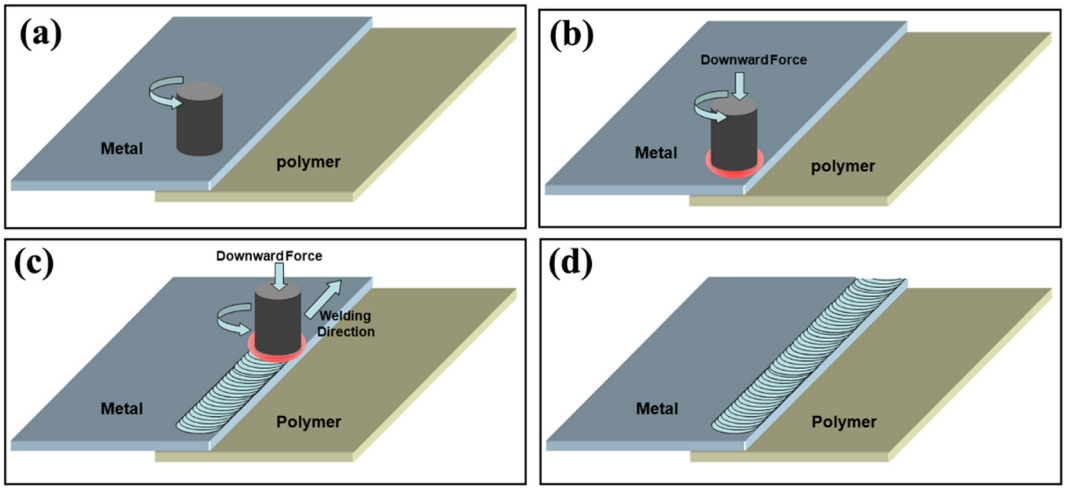

Fig 4. Schematic illustration of friction lap welding process.

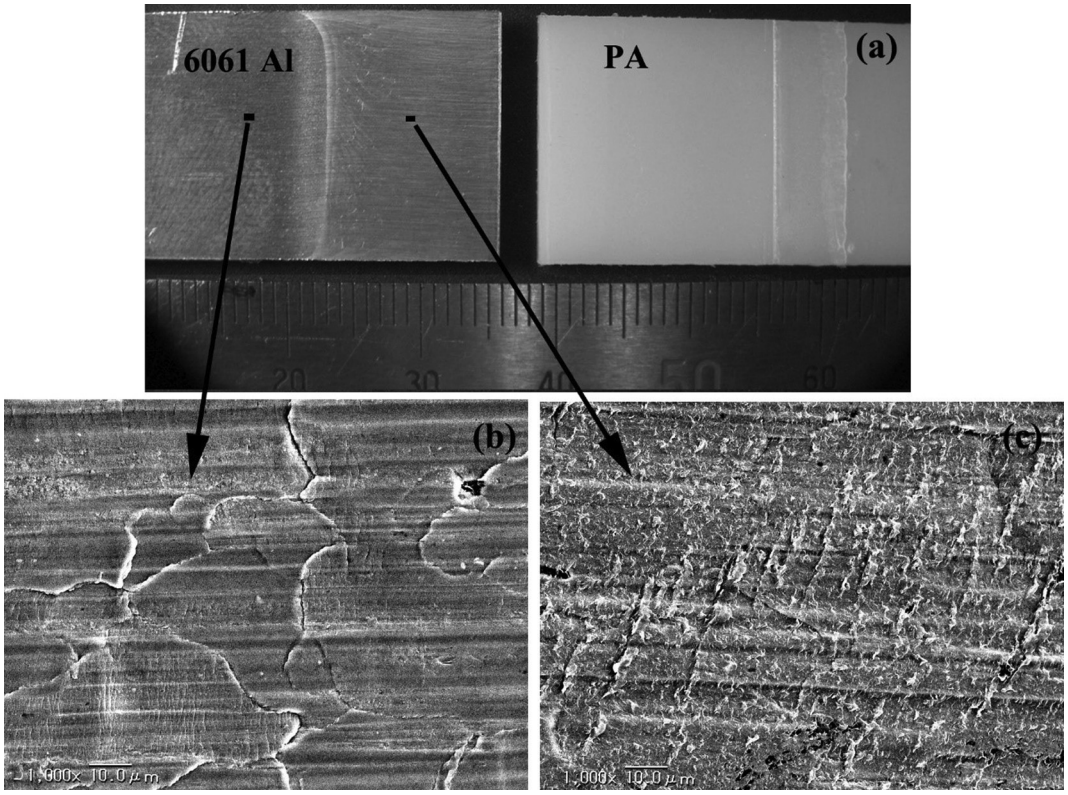

Fig 5. Fracture surface observation of lap joints of PA and 6061 Al produced by friction lap welding at 3000 RPM and 1500 mm/min: (a) optical observation of the fracture surfaces, (b) surface of as-received 6061 Al, and (c) fracture surface of 6061Al with a high volume of residua nylon.

strated that a linear relationship exists between H and $(R/V)^{0.5}$ when joining AZ31B Mg alloy to the polymer sheet. The welding temperature at the joint interface needs to be high enough to generate mechanical interlocking and/or chemical bonds between metal and polymers. However, overheating will cause polymer pyrolysis and form bubbles at the joint interface. These bubbles have no load-bearing capability and increase stress concentration under loading conditions. The dissimilar joints containing a high level of bubbles will not be accepted in critical structural applications. Liu et al. found that an appropriate increase in welding speed, tool rotation rate, and tool plunge depth can significantly reduce the volume of the bubbles [60]. Recently, Liu *et al.* [66] have shown that friction lap welding can conduct at a welding speed as high as 5 m/min and the produced joints are almost free of bubbles.

The strength of the joints produced by friction lap welding can be affected by many factors, including material combinations, surface conditions, and welding parameters. More investigation is necessary to fully understand the joining process and affecting factors. Without any surface modification, the nominal shear strength of lap joints of PA and 6061 Al produced by friction lap welding can reach 8 MPa [58]. When the Al surface was treated by silane coupling before joining, the nominal shear strength of lap joints of PA-based CFRP and 6061 Al produced by friction lap welding can reach 19 MPa [61].

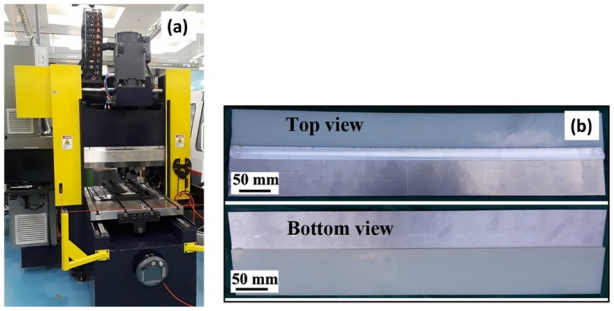

Fig 6. (a) A three-axis friction lap welding machine for joining process development. (b) The surface of a friction lap welding joint of PA and 6061 Al.

Friction lap welding can be performed using friction stir welding machines, milling machines, or purpose-designed equipment. Fig. 6a shows a three-axis friction lap welding machine for joining process development. The forces and torques associated with friction lap welding are relatively low comparing to friction stir welding and therefore the friction lap welding process can be implemented with an industrial robot for process automation. The joining speed can be as high as 5 m/min [67]. The processing time for a half-meter-long joining only needs approximately 6–8 seconds. A typical lap joint of 6061 Al and PA produced by friction lap welding is shown in Fig. 6b. No significant distortion was observed.

2.3. Friction Riveting

Friction Riveting (FricRiveting) is a process developed for joining metallic rivets with polymeric or composite parts. As a result of Friction Riveting, rivets are anchored within their joining partners in various possible configurations, while being deformed during this process, as a consequence of the applied joining parameters. The process is based on the combined principles of mechanical fastening and friction welding. The joining mechanisms are an interaction of mechanical anchoring and adhesive forces (if thermoplastic polymers or thermoplastic-matrix composites are joined), depending on the type of polymeric material(s) to be joined and their structural changes caused by the processing [68]. Namely, although possible to join thermosetting polymeric materials via Friction Riveting, such joints might only be limited to rely on adhesive forces, depending on the additives used. Micromechanical interlocking can also play a role in the strength of Friction Riveted joints, as the crevices formed at the surface of the deformed tip of the metallic rivet can be filled with molten and recured thermoplastic polymer [68,69]. The contribution of each joining mechanism to the global mechanical performance depends on the material combination and is subject to ongoing research.

Friction Riveting was developed and patented at the Helmholtz-Zentrum Geesthacht [70]. The equipment used can be installed on either commercially available friction welding spindles or more sophisticated laboratory equipment [68]. Furthermore, recently other researchers successfully performed and studied Friction Riveting by adapting devices and machines such as friction welding, milling, or drilling equipment [71,72]. The Friction Riveting process involves a high-speed rotating metallic rivet, which is plunged into the polymeric joining partner. In the stage of feeding and insertion of the rotating rivet, frictional heat is developed (the description of frictional heat generation and heat input model for the process can be found in [73,74]. The low thermal conductivity of the polymer in combination with the high thermal conductivity of the metallic rivet leads to a heat concentration at the rivet tip and the subsequent local achievement of plastic deformation temperatures (40–95% of the metal's melting point). The rivet tip deforms and anchors within its polymeric joining partners. The shape of the deformation tends to assume a parabolic shape but is also subject to the interaction with the structure of the surrounding polymeric or composite material and can be influenced by composite stacking sequence, fiber reinforcement material, composite inhomogeneity, among others [68]. Fig. 7 shows a schematic of the Friction Riveting process on the example of an overlapped CFRP/CFRP-Titanium Ti6Al4V material combination.

The process can be phenomenologically divided into two phases: the friction phase and the forging/consolidation phase. The friction phase is the initial stage of the process, from the rotating rivet touch-up on the surface of the polymeric partner until the rotation is stopped. The generated heat can lead to rivet tip deformation, resulting in sufficient anchoring in the so-called single-phase Friction Riveting. In the second phase (or the forging/consolidation phase), the axial load applied on the rivet is increased to a targeted value to achieve a greater anchoring deformation or a joint consolidation. Once the targeted axial load is achieved, the rivet is kept under constant load conditions to limit void formations. This second phase is not mandatory but can provide greater anchoring and enhanced mechanical performance under dynamic loading. Depending on the equipment used, the main joining parameters are rotational speed, joining time, and joining the force. Process parameters can be divided into friction and forging/consolidation time/force, depending on the process variant. Process variants are referred to joint configuration, process control, and division of phases. Thus, among the available and already substantially studied and optimized Friction Riveting (FR) variants, there are direct-FR, force-controlled FR limited by displacement or joining time, single-phase FR, and low-speed FR [68,75,76].

Friction Riveting has been demonstrated to be feasible to a multitude of material combinations, through joining polymer or composites (thermoplastic and thermosetting polymers, and glass/carbon-reinforced polymer composites) to various metals (including aluminum, titanium, and stainless steels) for several applications in aerospace, automotive, and civil engineering [77]. As the main joining mechanism is the mechanical anchoring of the deformed rivet within the polymeric plate(s), the anchoring efficiency has been described

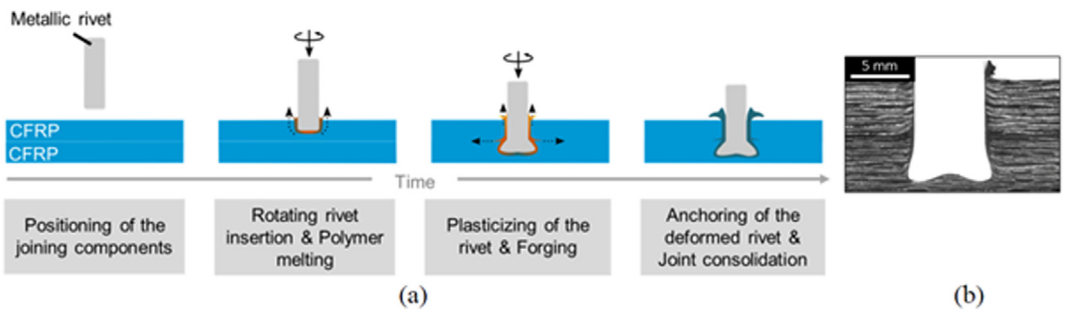

Fig 7. (a) Schematic illustration of the Friction Riveting process and (b) joint cross-section example of CFRP/CFRP overlap with a Ti6Al4V rivet (adapted from [69]).

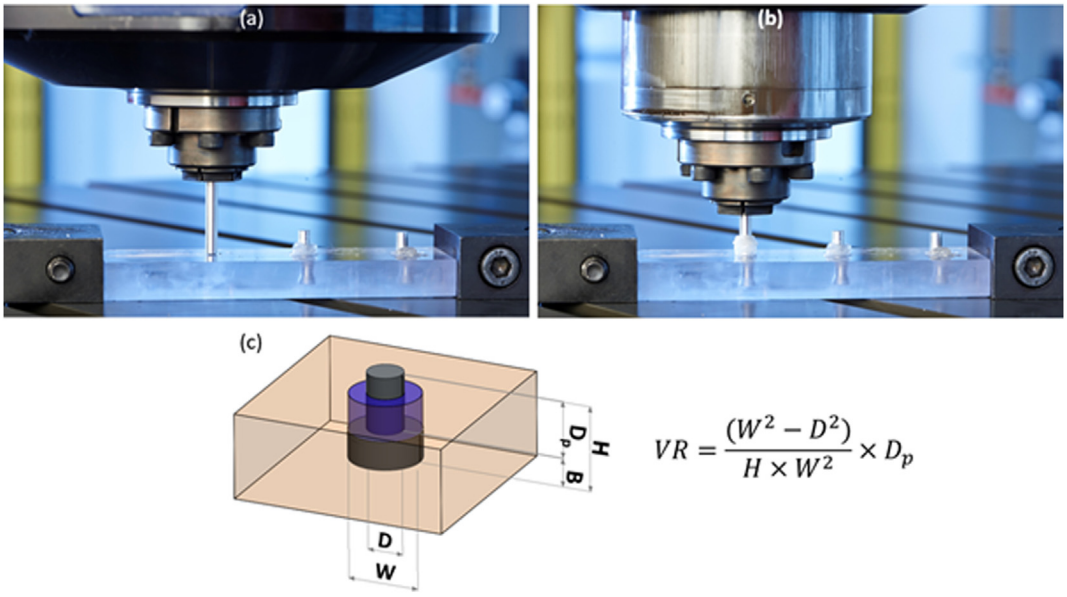

Fig 8. (a) Positioning of AA2024 rivet before the joining process with friction welding spindle on polycarbonate plate; (b) AA2024-T351/polycarbonate Friction Riveting joint; (c) concept illustration and equation for volumetric ratio (VR) calculation (a,b – courtesy of HZG/Christian Schmid).

as the volumetric ratio (VR), which qualitatively assesses the joint strength under tensile loading, taking into account only the geometry of the deformed rivet related to the remaining polymeric material above the deformed rivet tip opposing rivet extraction [78]. The VR does not provide sufficient information to assess the mechanical behavior under shear loading, with most of the potential applications studying overlap lap-shear configurations. Nonetheless, the VR provides sufficient data for guaranteeing a minimal out-of-plane resistance for lap-shear joints. In future research, the VR will have to be amended with material properties to establish strength equations for Friction Riveting. Extensive research has been conducted recently to determine the damage tolerance of Friction Riveting joints for aircraft applications, combined with the study of industry-relevant performance such as aging and corrosion. The process revealed a high potential for applications in the aircraft industry. Fig. 8 presents an actual AA2024-T351/polycarbonate joint before and after the process together with the illustration of the VR calculation concept, as expressed in [78].

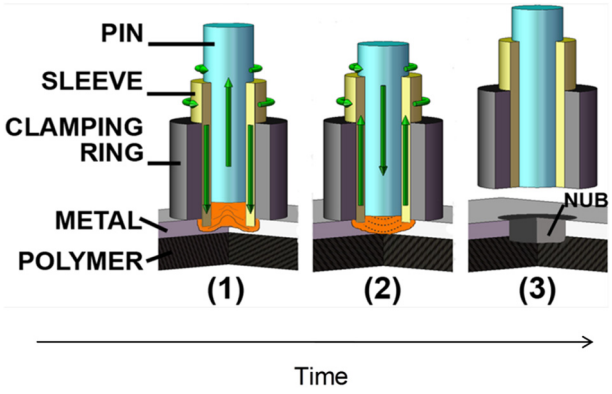

Fig. 9. Main steps of the FSpJ process in producing metal-composite overlap joints. (1) The sleeve plunges into the metallic sheet down to a predetermined depth, and the pin retracted in the opposite direction. (2) Pin and sleeve return to the metallic sheet surface. (3) The tools are removed, and the joint consolidates under clamping (fixtures and backing elements are not shown for simplification. Reproduced with permission from [33].

Besides the above-mentioned process variants, the Friction Riveting process has been successfully divided into several stages via differential controlling options using the dedicated laboratory equipment, with varying parameter settings during the insertion and forging. Therefore, Friction Riveting can be tailored and adapted for different joint configurations (including reduced or increased material thickness, multiple overlap sandwich structures, simple metallic insert joints, etc.). Nonetheless, one of the knowledge gaps is that most of the development and published work has been performed using rivets of either 4 or 5 mm thickness, both plain or with different tip geometries (threads, holes, etc.). The influence of a wider rivet diameter range on the process has not been thoroughly studied. The maximum joint strength achieved (published as ultimate tensile force and ultimate lap shear force) has been determined by the metallic rivet shafts when sufficient anchoring was guaranteed, which makes the process comparable to or even better than the state-of-the-art rivets or bolts with through-holes. The next steps in developing Friction Riveting shall be to upscale and downscale the process, and to assess the influence of rivet diameter on the joint formation and behavior, as these are in direct subordination to the industrial maturity of the technique. Important ongoing activities of Friction Riveting are the establishment of strength equations, and modeling of temperature development, and rivet anchoring zone formation.

2.4. Friction Spot Joining

The Friction Spot Joining (FSpJ) process was developed at the beginning of the 2010s [79] to join metals to various thermoplastic/thermoplastic composite (including unreinforced thermoplastics, fiber-reinforced thermoplastics, and woven-reinforced thermoplastic composite). As a further development of the so-called refill friction stir spot welding process (RFSSW) [80] for metals [81] and polymeric materials [82], the FSpJ process has been extensively described in [31–33,82]. FSpJ produces high-quality joints with the advantages of short joining cycles (2 to 8 s) and the absence of filler material and post-joining treatment [83]. Low-cost machinery and easy reparability are other advantages of this process. FSpJ process can be divided into three steps. In Step 1, the specimens to be joined are firstly clamped against a backing plate or bar (the latter when working with C-frame equipment). The sleeve and pin are driven to rotate in the

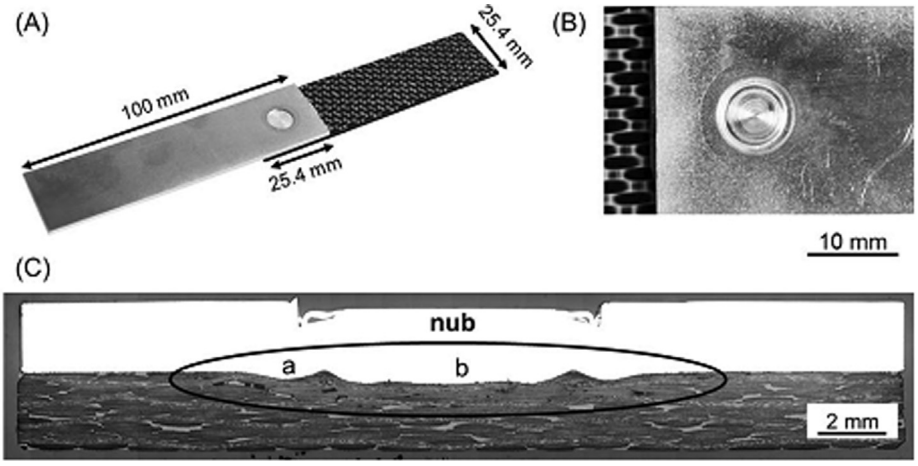

Fig 10. (A) Example of an AA7075-T6/CF-PPS friction spot joint along with typical (B) top view and (C) cross-section of the joints. The metallic nub is indicated with an ellipse in (C). The details of regions "a" and "b" are presented in Fig. 11. (Reproduced with authorization from [84]).

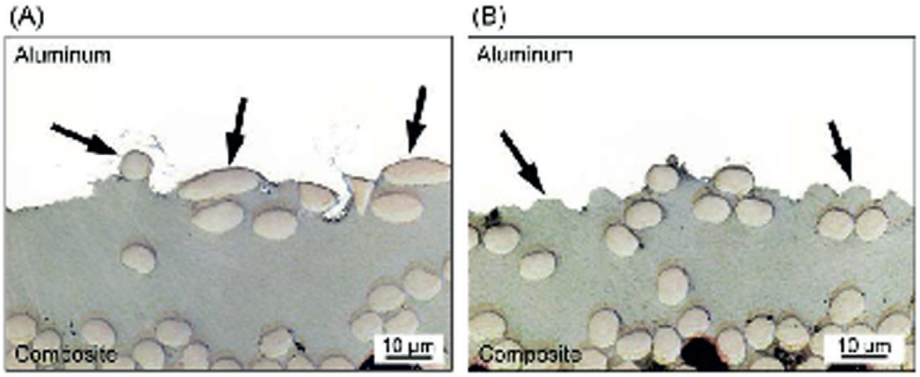

Fig 11. (A) Fiber anchoring (region "a" in Fig. 10) and (B) polymer matrix entrapment (region "b" in Fig. 10). (Reproduced with authorization from [84]).

same direction at a preset speed. The rotating sleeve plunges into the metallic sheet, and simultaneously the pin moves the opposite direction (Fig. 9-1), forming a cylindrical cavity that is filled with metal plasticized by frictional heat. The tool plunge depth is designed to be lower than the thickness of the metallic sheet to avoid the rupture of the fiber reinforcement, especially when woven-fiber reinforced thermoplastic composites are involved. In Step 2, the probe and sleeve return to the top surface of the metallic sheet. During its translation, the pin pushes back the plasticized metal, refilling the volume previously occupied by the sleeve during the sleeve retraction (Fig. 9-2). In Step 3, the tool set is removed from the metal surface, and the joint is consolidated without removing the clamping fixture until the welding temperature are lower than the glass transition temperature of the polymers (Fig. 9-3).

Fig. 10 A, B shows a typical AA7075-T6/CF-PPS single lap joint along with its top view. Joints present an excellent surface finishing. A representative example of the cross-section of these joints [83] is shown in Fig. 10C.

The two main bonding mechanisms responsible for the mechanical strength of the friction-spot joints are adhesive forces and mechanical interlocking [85,86]. The heat generated by the friction between the tool and the metal is transferred to the composite surface, promoting matrix melting/softening and consequently the formation of a polymeric molten film at the metal-composite interface. After joint consolidation, the solidified polymer induces strong adhesive forces – the first type of bonding mechanism in FSpP – which is critical for the shear strength of the joint. These adhesive forces can be molecular dispersive van der Waals forces (secondary forces at the interface, a phenomenon commonly called adsorption), or primary bonds (such as covalent, ionic, or organo-metallic, known as Chemisorption). As shown by Goushegir *et al.* [86], XPS analysis of the fracture surfaces of CF-PPS - AA 2024 aluminum single lap joints revealed that FSpJ leads to the formation of chemical bonds between the aluminum alloy elements and carbon from the molten PPS layer. Al–C was the primary chemical bond identified at the interface for both surface pretreatments [86]. The second type of bonding mechanism is mechanical interlocking. A representative example of the cross-section of these joints is shown in Fig. 10C (circulated with an ellipse). In the macroscopic scale, the slight deformation of the metallic sheet at the joint interface generates a geometrical undercut - a metallic deformation in the shape of two rings inserted into the composite part - known as "metallic nub". The slight insertion of the metallic nub into the composite was demonstrated to be able to increase the mechanical interlocking, and hence the shear strength of the joint, as shown by Andre *et al.* [84]. It is anticipated that the larger the volume of the nub, the larger is the micro-mechanical interlocking between the metal and the composite part, thereby higher volume of the composite entrapped into the nub and consequently a potential higher joint strength [83].

At the microscopic scale, micromechanical interlocking forms via filling the pores/crevices on the metal surface by the molten or softened polymer (Fig. 11B), which, after consolidation, increases the global shear strength of the joint [30]. Another important phenomenon was observed in the case of woven-reinforced composites: a portion

of the carbon fibers are entrapped by the plasticized metal, thereby creating a micromechanical interlocking (Fig. 11A) [30]. During the joining process, parts of the molten PPS matrix were squeezed out of the nub and was displaced by the softened metal. Under the action of the applied axial force by the sleeve and the pin, the plasticized metal penetrated the first plies of the composite, resulting in either individual fibers or fiber bundles being embedded into the metal [30]. These two phenomena of pore filling by molten polymer and fiber enclosure by the metal were shown to be largely responsible for the shear strength of the joints [84].

The main parameters of the FSpJ process are tool rotational speed (RS), plunge depth (PD), joining time (JT), and joining force or pressure (JF; JP). These process parameters directly influence the joining mechanisms and heat generation and consequently the microstructure and the mechanical performance of the joints. Briefly, the RS and the JT are the main process parameters controlling the heat generation (energy input) and the amount of molten polymer, as well as its viscosity [31–33]. Esteves *et al.* [31] and Goushegir *et al.* [32] found that the rotational speed of the tool had the highest influence on the lap shear strength of the joint, followed by the joining time, plunge depth, and the joining force. They showed that the RS and JT are responsible parameters for the heat input in the process; higher RS and longer JT decrease the viscosity and facilitate the flow of the molten PPS to spread in the bonding area [32]. The authors also observed that PD controls the micro-mechanical interlocking between the joining parts and influences the formation of the metallic nub. Goushegir *et al.* [32] studied the JF/JP, which was found to have a significant effect on the lateral flow of the molten polymeric matrix.

FSpJ has been used to join several combinations of materials. For example, FSpJ has been used to produce joints of AZ31 /glass-fiber- and carbon-fiber-reinforced polyphenylene sulfide (GF- and CF-PPS) [33] and AA6181 /CF-PPS, [31] for automotive applications. FSpJ has also been used to produce joints of AA2024-T3/CF-PPS [30] and AA7075-T6/CF-PPS [84] for aerospace applications. Recently, the process was also demonstrated its capability in producing carbon nanotube polycarbonate nanocomposites/AA6082-T6 single-lap joints in the automotive industry [87]. An attempt to qualitatively compare the FSpJ with the state-of-the-art welding-based joining technologies, including induction welding (IW), resistance welding (RW), ultrasonic welding (UW), and laser welding (LW), for producing metal-polymer hybrid structures was recently demonstrated in [84]. The produced joints with similar materials (metals and carbon-fiber-reinforced polymers), configuration (overlap), surface pre-treatments, thicknesses, and failure mechanisms to friction spot joints were compared. FSpJ joints showed comparable or superior quasi-static strength than the joints produced by the concurrent technologies, whereby nominal lap shear strength varied between 25 MPa and 65 MPa [84]. Another advantage of FSpJ is its shorter process times. FSpJ can produce a lap joint up to 4 s. In contrast, the induction welding process often lasts about one minute, while the resistance welding process needs to take from 30 s up to 5 min. The ultrasonic welding needs a short joining cycle similar to the FSpJ (3.5 s).

The quasi-static fracture behavior of a metal-composite FSp joint is governed by brittle fracture, similarly to the failure of adhesively bonded joints [32]. The micromechanisms of fracture demonstrated a mixture of ductile and brittle fractures. Three zones were identified on the fracture surfaces [88]: a smooth and featureless area demonstrating brittle fracture, a quasi-smooth area representing a mixture of ductile and brittle fractures, and finally a zone with a highly rough surface implying ductile fracture of the composite part. Furthermore, fiber pull-out and breakage were identified as additional fracture micro-mechanisms. Fig. 12 shows a fractured FSp Joint of AA2024-T351/CF-PPS on the composite part showing examples of the micromechanisms of fracture previously described. Both macro and micromechanical fracture behaviors were also reported to take place similarly under fatigue testing [89].

2.5. Ultrasonic welding

Ultrasonic welding/joining (USW) is a friction-based process capable to join dissimilar materials. The technology is particularly suited to join light metals to fiber-reinforced polymers, for example to weld Al and Ti alloys to glass or carbon fiber reinforced thermoplastics and epoxy composites [17,19,21,24]. Up to now, two options to weld metals to polymers by ultrasonics are available: the so-called “polymer welding variant” and “metal welding variant”. The main difference between the two is the direction of the ultrasonic oscillation. In the case of ultrasonic polymer welding, the vibration is parallel to the direction of the welding force and perpendicular to the surface of the sheets to be welded. For ultrasonic metal welding, the oscillation direction is parallel to the sheet surface.

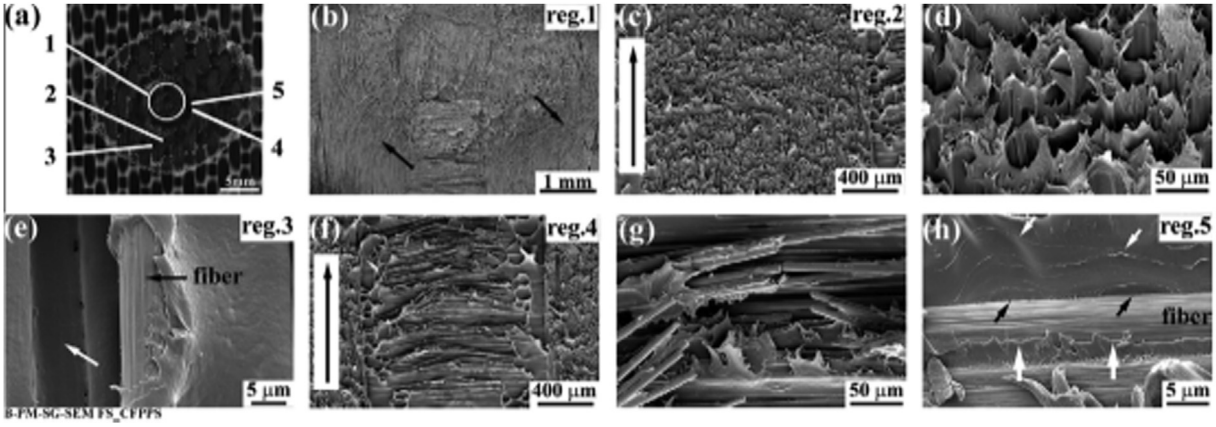

Fig 12. SEM fracture surface examination on the composite side from the regions indicated in (a), (b) general overview in the center of the spot where slight distortion of the fibers are indicated by the arrows, (c) elongated fibrils in an area containing warp fibers resembling a ductile fracture, (d) high magnification of the fibrils, where tearing fracture at the ends of the fibrils is apparent, (e) broken weft fibers, (f) high magnification of the broken weft fibers where slight rotation of the fibers in the direction of the applied load is visible. The direction of the applied load is indicated by the arrows in (c) and (f). (g) High magnification image of the warp fibers region in which the white arrow indicates an impression of a pulled-out fiber, and (h) high magnification image of the fiber–matrix debonding in a weft fiber as a result of weakened fiber–matrix adhesion. Black arrows indicate some micro-voids acting as crack initiation, small white arrows show crack propagation path, and large white arrows illustrate tearing fracture along with the fiber–matrix interface. (Reproduced with authorization from [88]).

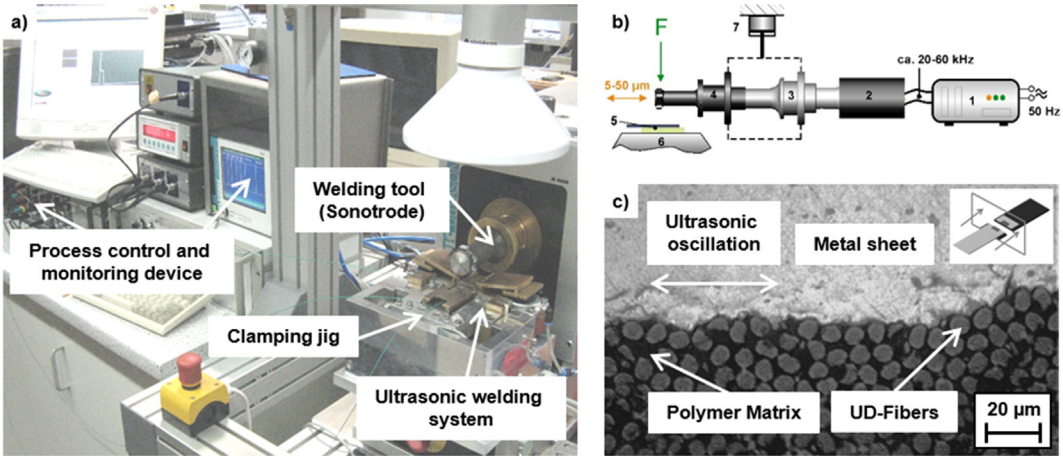

Fig 13. a) Experimental equipment for ultrasonic metal welding of metal/FRP; b) Main components of the welding system: Ultrasonic generator (1), piezoelectric converter (2), Booster (3), Sonotrode (4), Joining partner (5), Clamping jig (6), Load transmission (7); c) Characteristic interface area of an ultrasonically welded Metal/FRP-joint (metal welding variant).

Previous studies have shown that both methods apply to welding metals to FRP. By using the "polymer welding variant " techniques, the resultant joint interfacial area is characterized by fully adhesive contact between the metal and the polymer matrix and a reduced bonding strength lower than the shear strength of the chosen polymer matrix [21]. The highest mechanical properties were observed for the "metal welding variant" owing to the direct contact of the load-bearing fibers and the metallic surface. The formation of the hybrid bonds occurs as a result of moderate joining forces not higher than 500 N and a superimposed oscillation amplitude of 50 µm in maximum, at a frequency of 20 kHz, without reaching their melting points in the case of metals [23]. Furthermore, the welding process is characterized by a low energy input with less than 5 kJ, consequently low temperatures in the welding zone (less than 350 °C in case of aluminum) and very short welding times (less than 5 seconds) as well as moderate investment costs (less than 80 k€). Most metals can be ultrasonically welded in general. In case of metal to polymer composites joints, several Al wrought alloys (AA1050, AA2024, AA2198, AA5024, AA5754, AA7075), Ti alloys (cp-Ti, Ti64) were successfully welded to CFRP and GFRP laminates with different fiber textiles and polymer matrix like PA12, PA66, PPS or even PEEK. A typical experimental setup of an ultrasonic metal welding system for hybrid joints like metal to FRP joints is depicted in Fig. 13a.

Fig. 13b presents the main components of a metal welding system and Fig. 13c shows a typical joint interface between a metal and an FRP produced by the "metal welding variant". Enough plastic deformation is required to realize a direct contact between the fibers and the metal as well as a mechanical interlocking of the metal surface and the fibers. The needed energy for deformation is introduced by the high-frequency vibrations between the welding tool and the joining partner, which are fixed on an anvil or an adapted clamping jig. The sonotrode generally oscillates with amplitudes in the range of 5–50 µm, corresponding to local sliding velocity of more than 6 m/s at the sonotrode tip and 20 kHz welding frequency.

The design of the ultrasonic welding spot is flexible and allows areas of typically around 100–200 mm^2 with a rectangular or circular shape. The essential relative motion at the dissimilar material interface is provided by a resonant unit out of three main components: converter, booster, and sonotrode (see Fig. 13b). The mechanical oscillation is realized with the help of high-efficient piezo-ceramics. These main elements of the converter transform the high-frequency electrical oscillation of the generator into mechanical oscillation without significant losses in the range of 8 to 12 µm. Booster and sonotrode, which are mostly designed out of titanium or powder-metallurgical iron-based alloys, stabilize and transform the displacement amplitudes up to 50 µm by their single transmission ratio of 1:2 or even 1:3.

The major influencing parameters to realize high-quality hybrid joints are split into the process and material-related impacts. The major process parameters are the oscillation amplitude (u), and the welding force (F). The final major process parameter is the specific welding energy W_{US}, which is often used to control and complete the USW process by logging the generator power-time-function. Influencing factors corresponding to the materials to be welded are their mechanical and physical properties, including stiffness, hardness, and yield strength as well as geometrical limits like the maximum thickness of 2.5 to 3 mm for the upper sheets. The thickness of the lower joining partner, mostly the polymer composite laminate, is not of relevance for the process. The occurring temperatures during ultra-

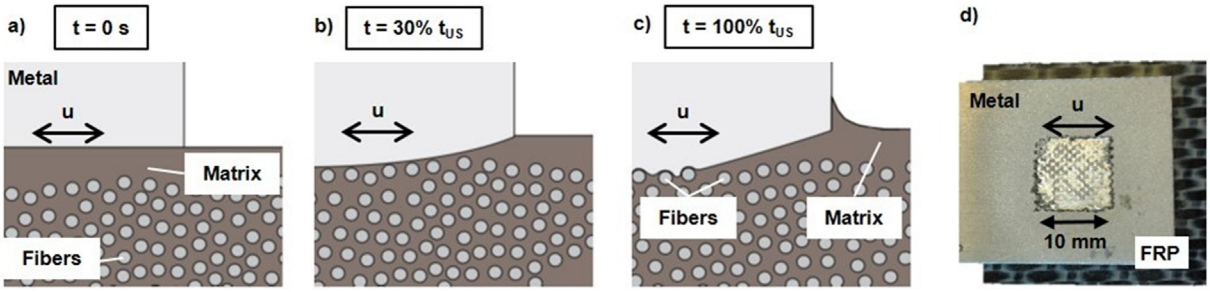

Fig 14. a-c Temporal sequence of bonding formation during ultrasonic metal welding of metals to fiber-reinforced thermoplastic composites, d) Ultrasonically welded Al/CFRP-specimen with characteristic tool imprint (adapted from [90]).

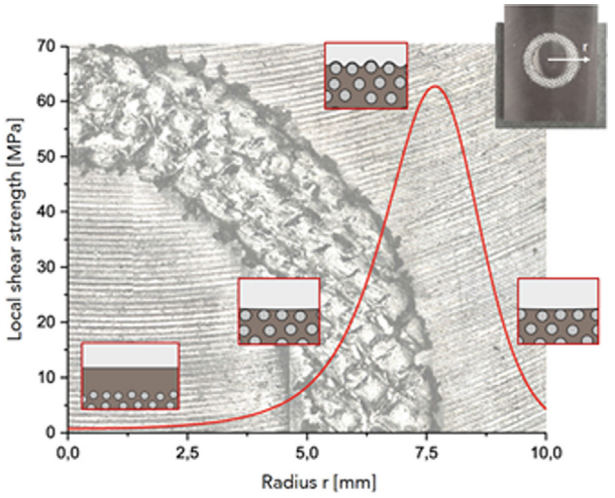

Fig 15. Local strength distribution of ultrasonically welded AA5024/GF-CF-PEEK joints as a function of distance r to the center of weld spot (Reproduced with authorization from [90]).

sonic welding of metal to FRP are affected by the process settings and the characteristics of the material in a similar manner. Although elevated temperatures can enhance the process, these are not essential to realize a strong interface.

The welding process of metal to fiber-reinforced polymers (FRP) by power ultrasonics can be divided into three main sequences, as pictured in Fig. 14a–c.

In the initial phase, sufficient welding energy as a result of the relative motion between the upper and lower joining partner enables the first connection. In this stage, the polymer adjacent to the interface melts. The molten polymer is displaced out the area underneath the sonotrode tip up to the upper fiber ply (Fig. 14b) after approximately 30% of the entire process time. At this time, the hybrid bond is purely adhesive corresponding to tensile shear forces in the range of 25% of the maximum achievable shear strength [24]. During the main sequence of the process, pronounced plastic deformation of the metal sheet takes place and the maximum temperatures reached 250–350 °C. The melting of the polymer between individual fibers enables a direct fiber to metal contact as well as mechanical interlocking by local yielding of the ductile metal at elevated temperatures (Fig. 14c). Nevertheless, no polymer decomposition or fiber fracture was noticed due to the moderate process temperatures as well as ultrasonic oscillation parallel to the fiber orientation.

The contribution of adhesive and cohesive to bond strength was studied using special welded samples prepared through intermittent ultrasonic welding. Fig. 15 summarizes the local shear strength as a function of the distance to the center of the weld spot. The direct Al/Fiber connection resulted in a high local joining strength of 60 MPa at the outer radius of the welding spot (r = 7.5 mm), i.e. the area directly underneath the sonotrode tip. The integral of the strength curve represents the measured total force of the welded hybrid joint with 8500 N on average. Further details and findings by interrupted welding experiments are described in [24].

3. Friction-based process characteristics

This section is aimed at describing the advantages, issues, and challenges facing the friction-based joining processes used for metal-polymer and metal-composite structures. Besides, a comparison among the processes in terms of the joining force, power as well as heating mechanisms according to the current states of the technologies is summarized. The summary is not designed to define the boundary of the joining technologies as the limitation of the process are still under exploration.

3.1. Advantages of the friction-based welding process

Most of the friction-based processes share the following major advantages:

- Very short joining time, (typically between 0.5 and 10 s);
- Reduced number of installation steps, with no pre-drilling required;
- Little or no surface preparation is required, thus environmentally friendly;
- Suitable for various joint types (spot, linear and curvilinear);
- High joining speed for long continuous joints (can be as high as 5 m/min);
- Single-sided-access and hermetically sealed joints;
- Reduced stress concentration due to the avoidance of through-holes;
- Versatile process, multiple material combinations possible;
- Easily automation and integration with robotic systems;
- High joints strength;
- High energy efficiency;
- No need for shielding gas and special protection;
- No sparks, glare, or electromagnetic hazard during the process;

3.2. Main process differences

Table 1 summarized the joining power and force needed for each joining process. Friction-assisted joining and friction lap welding do not involve a significant tool penetration into the components but need to apply rapid rotational friction on the top surface of the metal to be welded under relatively high pressure. In contrast, friction spot joining and friction riveting need a deep tool penetration into at least one of the components to be joined. It is easy to understand that friction spot joining and friction riveting need a relatively higher joining force and power than friction-assisted joining to produce a joint of the same size. Since either friction spot joining, friction riveting, or friction assisted joining can be coupled into a C-frame, none of these processes need a welding machine with a high requirement on stiffness for most of the applications, making these processes attractive for assembly line applications. Friction lap welding can produce strong metal-to-polymer hybrid structures at low forging force and power when high welding speed is not critical. When the process needs to be completed at high welding speed (such as 5 m/min), the applied joining force and power need to be increased correspondingly. Compared with friction-assisted joining, ultrasonic welding needs less joining force but higher joining power. This may be associated with the fact that ultrasonic welding requires sufficient power to vibrate one of the components to be welded.

Table 1
Joining force and process power demands of friction-based joining processes.

	Indirect Heating			Direct Heating	
	Friction Assisted Joining	Friction Lap Welding	Friction Spot Joining	Friction Riveting	Ultrasonic Welding
Joining force, Peak [kN]	1–2	1–10	2–6	1.5–10	Up to 0.5 kN
Joining Power [kW]	0.5–2	0.1–0.5	Not available	1.85–30	0.5–10

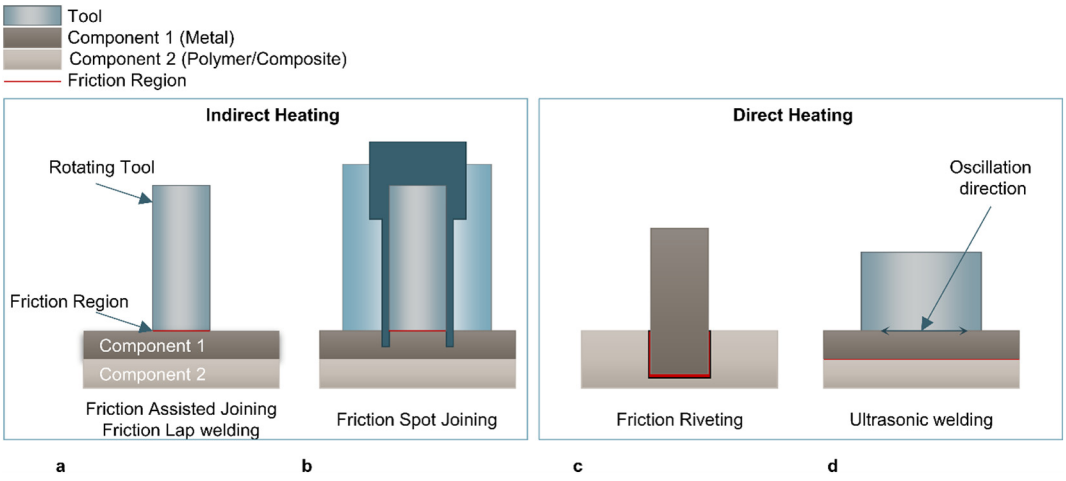

Fig 16. Classification of the processes based on indirect and direct frictional heating.

Friction-based joining processes can be achieved through either a direct heating system or an indirect heating system, as summarized in Table 1 and schematized in Fig. 16. Using direct heating systems, the frictional heat is generated directly at the joint interface. Thus, friction riveting and ultrasonic welding belong to this category. In the case of ultrasonic metal welding, the bonding is promoted by the relative motion between the metal and the FRP sheet. Therefore, the interfacial bond can take advantage of the plastic flow of ductile light alloys (Al, cp-Ti) and subsequently lead to a combination of the mechanical interlocking and a direct atomic-level bonding between the metal and the FRP [90]. Friction-Assisted joining, Friction Lap Welding, or Friction Spot Joining, produces frictional heat at the interface between the external joining tool and one of the components to be joined (typically the metal counterpart). Thus, the heat is not directly applied at the joint interface but through heat diffusion via one of the components to be welded. Indirect heating less efficient than direct heating processes in theory since a larger amount of material (the entire thickness of the metallic component) needs to be heated up before the desired temperature can be achieved at the metal-polymer interface. Indirect heating involves some heat loss owing to the heat diffusion towards the surrounding material [52] which may lead to less energy efficiency. longer joining time (as a larger amount of energy is required), as well as larger heat affected zones (this may affect the behavior of semicrystalline polymers). In reality, the high tool rotation rate allows high power density and therefore significantly reduced joining time, and less heat loss and energy waste. Also, the energy waste in indirect heating systems will increase with for thicker the metallic component due to the increased distance between the heating source and the joint interface.

3.3. Process design and control

The joining development is highly influenced by the temperature achieved at the metal-polymer interface. Thus, it would be of great interest to measure and/or predict the temperature evolution at the metal-polymer interface. However, the whole picture of the temperate distribution at the interface is hard to be obtained using either contact or non-contact measurement equipment. Thus, a suitable approach would be the adoption of a numerical model that is capable to predict the temperature evolution and distribution during the process, as reported in [91]. Besides, during friction-based joining processes, as the steep variation of the temperature, processing conditions change significantly. An example is reported in [92] in which linear friction stir welding of aluminum alloys was analyzed. In the beginning, the tool is in contact with a cold material (with high yield stress) and high contact forces develop. This also involves high frictional force produced at the interface. The frictional heat was produced as the process proceeds, which leads to a significant temperature rise of the material. This leads to the reduction of the flow stress, which consequently involves the reduction of frictional heat provided. Similar conditions also develop during Friction assisted Joining (FaJ). Even at a constant tool rotation speed and plunging load, significant variation of the welding power was observed [55]. These issues are very complex to be modeled through closed-form equations owns to the following factors:

- the variation of the flow stress of the upper and lower material;
- the variation of the tool temperature during the process
- the variation of friction conditions between the tool and the upper sheet;
- the variation of heat exchanges: conductive, (towards surrounding material, and the clamping frame);
- convective and radiation (towards the external environment).

The difficulty in accounting for all these factors lead to the adoption of Machine Learning tools for process design and control. An example is reported in [93], where a predictive model developed for temperature forecasting is based on power measured during the process. The model was capable to predict the temperature evolution based on the actual temperature and previous values of temperature. In this way, the model was capable to predict the temperature evolution during friction-assisted joining.

3.4. Surface pre-treatments

Although not compulsory, the use of surface pre-treatments, such as those adopted in adhesive bonding, can further improve quasi-static strength. Goushegir *et al.* [94] evaluated the influence of various aluminum surface pre-treatments on the bonding mechanisms and mechanical performance of the metal-CFRP joint produced by FSpJ. Chemical (Acid pickling etching and conversion coating) and electrochemical (phosphoric and sulfuric acid anodizing) treatments led to the formation of strong chemical primary bonding between the metal and composite. Phosphoric acid anodizing with an additional primer layer showed the best performance in increasing the joint's strength [94]. The reason was that the strong bond formed between the primer layer and the matrix of the composite during the joining cycle. Goushegir *et al.* [89] showed that fatigue performance can also be improved by the application of these metallic surfaces pre-treatment, following the same trends observed for the quasi-static mechanical testing. More-

over, the author showed that the fatigue performance of the spot hybrid joints at 10^5 cycles (a standard procedure normally adopted to evaluate new joining techniques in aviation) was 47% of the quasi-static ultimate lap shear force (ULSF), which was higher than that of ultrasonic welding (32% ULSF).

Andre *et al.* [95–97] analyzed the influence of plasma treatment on the mechanical performance of FSp joints produced with a polymeric interlayer film. The authors observed an increase of 20% to 55% in ULSF after adopting an interlayer film [95], due to the larger bonding area, better load distribution, and improved micromechanical interlocking at the interface. Plasma activation usually enhances the composite adhesion, mainly due to the increase of surface energy. The plasma oxidizes the polymer surface, leading to the removal of organic contaminants and the introduction of polar functional groups [98]. Therefore, more reactive and wettable surfaces can be created, theoretically leading to stronger metal-composite joints. However, this positive phenomenon was not observed in FSp joints without the use of interlayer film, whereby the plasma activation did not increase the strength of the FSp joints. The reason for this behavior was correlated with the very thin surface layers of the functional groups created by the plasma (depths from several to tens nano meters) which were destroyed during the frictional melting of the composite interface.

Impact resistance of the FSp joints has been investigated. Andre *et al.* [99] studied the impact resistance of the joints of aluminum alloy 2024-T3 and carbon-fiber-reinforced polyphenylene sulfide using a drop weight test. The impact was applied on the aluminum-side and composite-side, respectively, to provide a preliminary understanding of the impact resistance of the joints. Four energy levels were used: 2 J, 4 J, 6 J, and 8 J. The joints that were impacted from the aluminum side presented residual strengths of 84% (2 J), 30% (4 J), and 25% (6 J). For composite-side impacted joints, the residual strengths were 80% (2 J), 54% (4 J), and 45% (6 J). Generally, the impact on the aluminum side leads to lower residual strength. The impact energy introduced from the aluminum side was mostly absorbed by the plastic deformation of the aluminum part, which bent the aluminum and promoted the detachment of the interface. In contrast, the impact energy introduced from the composite side was mostly absorbed by the creation/extension of internal damage of the plies of the composite. Thus, the authors [99] showed that the impact energy was only partially transferred to the interface of the joint in the case of applying impact from the composite-side. Consequently, these joints presented higher residual strength after impact than the joints impacted from the aluminum-side.

Goushegir *et al.*[100] investigated the durability of the aluminum-to-composite friction spot joints and their behavior under harsh accelerated aging as well as natural weathering conditions. Four aluminum surface pre-treatments were selected to be performed on the joints: sandblasting (SB), conversion coating (CC), phosphoric acid anodizing (PAA), and PAA with a subsequent application of primer (PAA-P). Most of the pre-treated specimens retained approximately 90% of their initial as-joined strength after accelerated aging experiments [100]. In the case of the PAA pre-treatment, the joint showed a lower retained strength of about 60%. This was ascribed to the penetration of humidity into the fine pores of the PAA pre-treated aluminum, reducing the adhesion between the aluminum and composite [100]. Moreover, the friction spot joints produced with three selected surface pre-treatments have been holden outside under natural weathering conditions for one year in Geesthacht, Germany. PAA-P surface pre-treated specimens demonstrated the best performance with a retained strength of more than 80% after one year. The authors ascribed this behavior to the tight adhesion at the interface and the chemical bonding reduction caused by the penetration of humidity into the interface between the joining parts [100].

The influence of engineering corrosion on AA2024-T351/CF-PPS Fsp joints [83] and AA2024-T351/CF-PPS Fsp joints was investigated by André *et al.*[101]. The engineering corrosion analysis was carried out on joints exposed to salt spray for one to six weeks. According to the observation on the top surface of the joints, the aluminum part corroded preferably in the heat-affected zone (HAZ). The authors demonstrated that the HAZ is more susceptible to corrosion than the stir zone (SZ) which is dominated by dynamically recrystallized grains. This is because the anodic sites formed around coarse intermetallic particles and S'(S) phase precipitation [101]. Besides, the macro-galvanic coupling between the zones may also potentialize the corrosion in the HAZ as the base material and the SZ displayed a lower volume fraction of S'(S) phase precipitation than the HAZ [101]. Moreover, the corrosion at the interface of the joints was evaluated. Four different stages in the development of corrosion at the interface were identified and the residual strength of these joints was assessed using a lap shear test. At Stage I, the joints showed fast strength degradation (0% to −24% of ULSF) due to water absorption and NaCl migration into the composite [101]. At Stage II, the strength degradation of the joints was stalled (−24% to −28% of ULSF) due to the protection provided to the bonding area by the reconsolidated layer of the polymer at the borders of the joint [101]. The polymeric layer acted as a protective coating on the aluminum surface. At Stage III, the corrosion overcame the polymeric layer by reaching the center of the joint. As a result, the strength of the joints rapidly degraded from −28% to −44% of ULSF [101]. Finally, at Stage IV, generalized corrosion took place, leading to the final strength degradation of the joints [101].

4. Discussion

The development of new joining processes suitable for hybrid metal-polymer and metal-composite structures is becoming a major research challenge since the broad employment of hybrid structures. Conventional joining processes such as mechanical fastening and adhesive bonding are characterized by severe limitations. Recent developments in this field are focusing on the direct combining of the components through thermomechanical joining processes. Among them, friction-based joining processes have demonstrated their capability in producing high-performance joints with a short joining time. Compared to adhesive bonding, these processes enable higher performances, higher standardization, easiness of automation, shorter joining time, and minor environmental impact. Besides, all these processes produce a relatively smooth surface, while the opposite surface (polymer or composite sheet) remains unaffected. This aspect is particularly interesting if comparing them to most of the mechanical fastening processes, which generally involve parts of the connection elements that protrude from both sides of the joint. Another common advantage of friction-assisted joining processes (except for friction riveting) is free of a connecting element, which contributes to weight reduction.

A direct comparison of the joining methods is hard due to the great difference in process maturity, e.g. friction spot joining was patented almost ten years ago, while the first study concerning friction assisted joining was performed only in 2017. This difference is also evident in Table 2, which reports the main analysis performed on the joints made by different processes. It is clear that, in almost ten years friction spot joining, friction riveting, and ultrasonic welding have reached a good degree of maturity. On the other hand, more recently developed joining processes such as friction lap welding and subsequently friction assisted joining require more efforts for researchers to provide a more comprehensive understanding.

Some industrial application proposals have been developed for processes such as friction riveting and friction spot joining, which are characterized by greater maturity. The upscaling of the technologies was investigated by André [83] (FSpJ) and Zocoller Borba (Friction Riveting) [102]. In a team effort, the authors co-produced a prototype of an aircraft fuselage part using FSpJ as one of the joining methods. The produced component was a hybrid metal-composite skin rein-

Table 2
Degree of process maturity.

	Friction Assisted Joining	Friction Lap Welding	Friction Spot Joining	Friction Riveting	Ultrasonic Welding
Shear Tests	YES	Yes	YES	YES	YES
Peeling/Pullout Tests	NO	NO	YES	YES (pullout)	NO
Numerical simulation	NO	NO	YES	YES	YES
Dynamic/Fatigue tests	NO	NO	YES	YES	YES
Chemical/environmental tests	NO	NO	YES	YES	YES (aging)
Applications (Functional prototypes)	NO	NO	YES (metal stringer to composite skin)	YES (stringer to skin panel, Omega stringer runouts)	YES (Omega stringer, Hybrid open profiles)

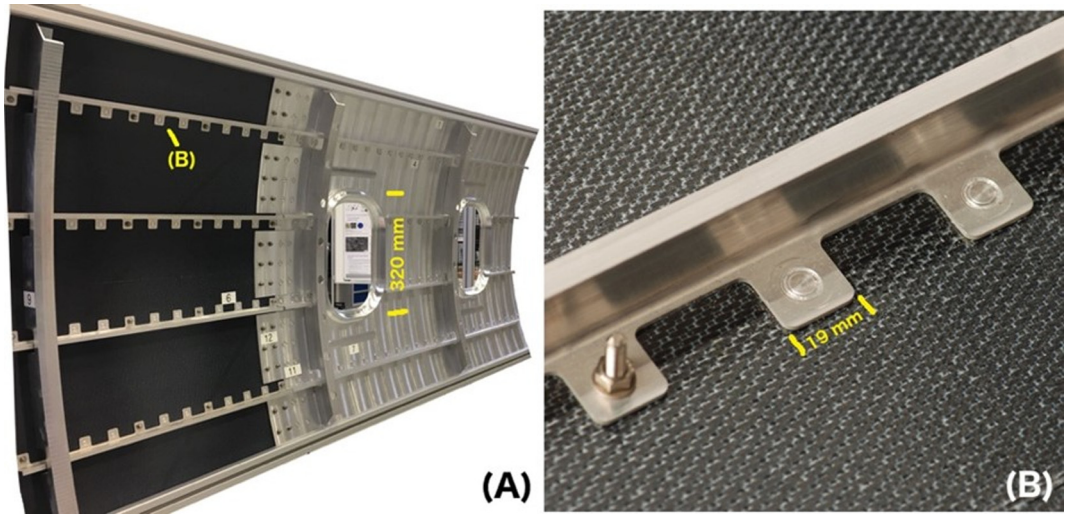

Fig 17. A) Overview of the metal-composite demonstrator produced entirely with friction-based joining technologies at HZG Germany. (B) composite skin-metallic stringer joined by two FSp joints and one friction-riveted joint.

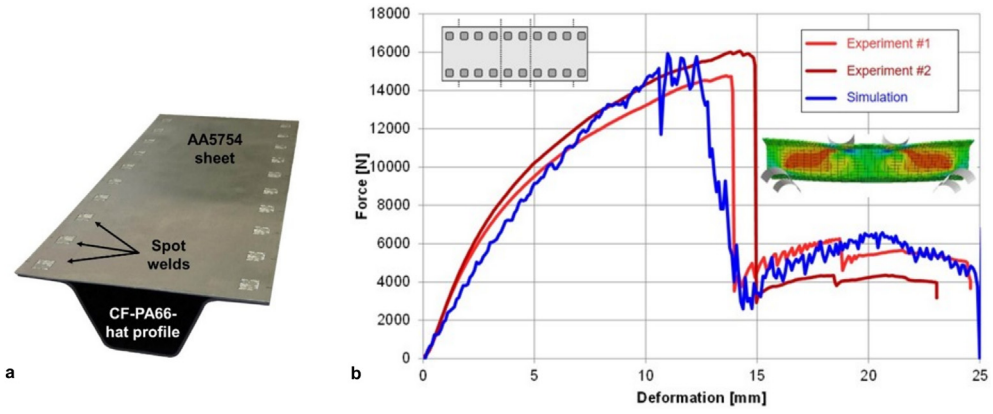

Fig 18. a) Ultrasonically multi-spot welded Al/CF-PA66 structure, b) Comparison of mechanical performance by experiment and simulation (Reproduced and adapted with authorization from [103]).

forced with metallic stringers and frames (Fig. 17A). The skin of the part consisted of a hybrid combination of 3.4-mm thick AA2024-T3 and CF-PEEK (carbon-fiber-reinforced polyether ether ketone) curved panels, while the stringers consist of 1.6-mm thick AA7050-T7. Friction spot joining was used to join the stringers to the composite skin, as depicted in Fig. 17B. The elimination of traditional fastener connections throughout the hybrid structure supported, among others, by the FSpJ technique provided an 8% decrease in the structural weight (around 2 kg).

Preliminary demonstrators were also developed for hybrid metal-composite joints made by ultrasonic welding on relatively complex (omega) geometries, as shown in Fig. 17. The chosen geometry of the multi-spot-welded hybrid demonstrator is following structural parts of an airplane fuselage section or chassis parts of a car body. The aluminum-magnesium wrought alloy AA5754 (thickness of 1 mm) was welded to thermo-formed CFRP laminates with polyamide PA66 matrix (2 mm thick). Up to 20 weld spots (each $10 \times 10\ mm^2$) were realized and their mechanical performance was evaluated by 4-point-bending tests. By hybrid welding, the profile is no longer an

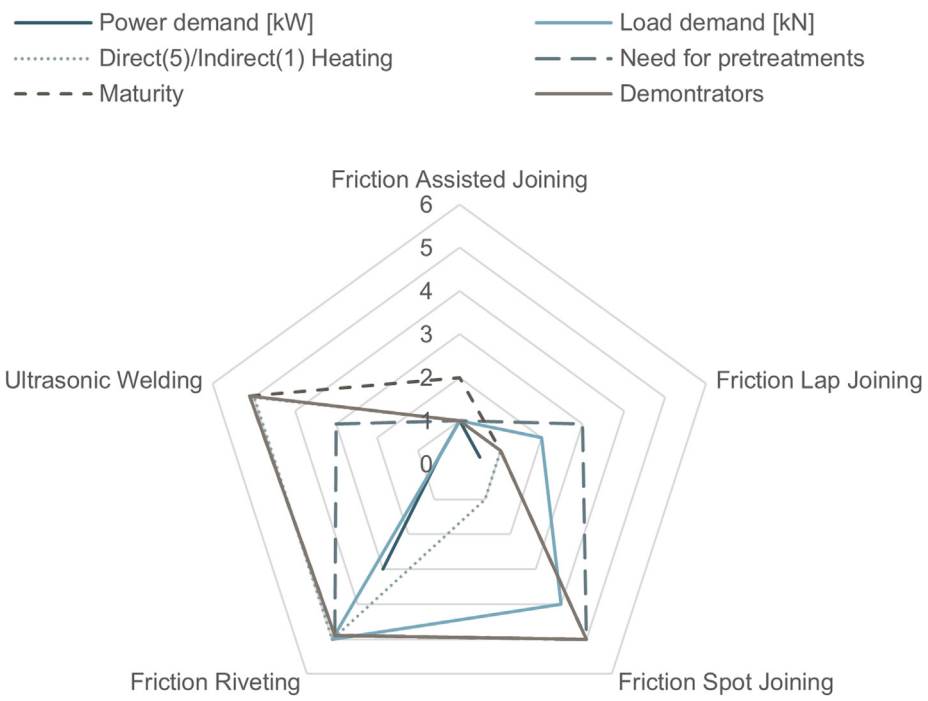

Fig 19. Schematic of main differences among friction-based joining processes.

open profile, and the stiffness, strength, and maximum deformation rise enormously. Thus, after a linear load increase (Fig. 18b), a non-linear curve section up to the maximum loads of up to 16 kN is followed. The failure of all spot welds causes a significant drop down to the level of the now open profile. Further details and results are given in [103].

The main differences for the joining methods regarding load and power demand, the position of the heating system, need for pretreatments, and maturity are schematically summarized in Fig. 19. As discussed before, the low power demand and load demand of some processes (especially for friction-assisted joining and ultrasonic welding) would enable small, lightweight, and even portable machines. The need for pretreatments, which are mandatory for some applications may represent a limitation and would require additional work for the joints fabrication. The comparison in terms of maturity underlines that friction-assisted joining and friction lap welding requires a step forward to understand their behavior when the joints are loaded in different directions or subjected to dynamic loads. Besides, the long-time variation of the load-bearing capability should be monitored as well as when the joints are immersed in a chemically aggressive environment.

Despite these differences, most friction-based processes are facing similar challenges. Some of the improvements introduced for one process are likely to be effective for the other processes. For example, recent advances in metal surface pretreatments (used to improve mechanical strength) would be beneficial for almost all friction-based joining processes. Besides, the challenges of directly measuring the metal-polymer temperature and the fine control of the temperature field during the joining process need to be overcome. These would allow achieving the optimal temperature at the interface, controlling the joint dimension, and avoiding adverse phenomena that develop at excessively high temperatures. This would also improve energy efficiency and reduce the joining time. To this end, the numerical model developed in [91] or the machine learning forecasting model reported in [93] for friction-assisted joining could be easily extended to other friction-based processes. Similarly, the pre-treatments used in friction spot joining and friction lap welding could be effective when extended to the other joining processes.

In the light of previous considerations, to push friction-based joining processes from laboratories into industries, some issues should be addressed, as follows:

1. Provide a clearer understanding of the influence of different surface pre-treatments on the joints quality;
2. Identify the main bonding mechanism directly influencing joint mechanical performance to further improve the technological readiness level of friction-based joining technologies. Develop novel manufacturing methods or procedures to amply the effects in a cost-effective manner.
3. Establish the relationship of processing thermal cycle, joining pressure, and duration on the bonding quality.
4. Develop reliable forecasting tools that enable to predict the fast evolution of the process-related temperature and material flow;
5. Develop reliable approaches that account for the characteristics of the involved material and enable an engineered process design and optimization. This approach would benefit from the predicting tools described at point 4, and could easily explore different processing condition sets to identify the optimal processing window, which maximizes a given objective function. This could dramatically reduce the time and cost-consuming phase generally represented by a fully experimental approach.
6. Provide online process control systems that are based on the current measurement of processing signals (e.g. temperature, processing forces, etc.), and the involved materials, can automatically adjust the joining program (e.g. varying the duration of the different phases or processing speeds during the process).
7. Develop hybrid joint quality evaluation, certification methods, and standards for future high-volume production environments.
8. Enable sustainable technologies for closed-loop material cycles to join, separate and repair multi-material structures and to address resource-wasting by material- and energy-efficient processes.

5. Conclusions

This article presents a detailed review of recent advances in friction-based joining processes employed for hybrid metal-composite joints. The main joining mechanisms, tested materials, and mechanical performances of the hybrid joints produced by different joining processes including friction-assisted joining, friction lap welding, frication spot joining, friction riveting, and ultrasonic welding have been discussed. The main differences among these processes were explored in terms of the joining force, power, heating mechanism, required surface pretreatments as well as process maturity were analyzed. Similarly, the main common advantages of the joining processes were analyzed and discussed, including the high strength of the joints, low processing time (typically less than 5 s), easy automation, high energy efficiency, etc. All the friction-based joining processes provided comparable or higher strength than adhesive bonds. Thus, the friction-based joining process represents a suitable alternative for manufacturing future multi-material lightweight structures.

Friction-based joining processes have many common issues that demand an interdisciplinary approach involving physical process development, materials science, thermo-mechanical engineering, and control system design. The strength of joints made by these processes is strongly dependent on the temperature evolution at the joint interface. However, since frictional power is used to heat (through direct or indirect heating) the components' interface, the frictional power changes during the process owing to the softening of the involved materials at elevated temperatures. This further complicates the process design and control in terms of the selection of processing time. To this end, recent studies involving numerical models and machine learning approaches have been conducted. These approaches could represent a suitable way for process design, parameter optimization, and control of friction-based joining processes. Similarly, the coupling surface state of the components represents a common issue for these processes. The study also pointed out a great difference in terms of process maturity. While some processes, which were developed at the beginning of the previous decade, have been thoroughly tested up to the development of preindustrial prototypes, some recently developed joining technologies have demonstrated their potentials but require further comprehensive analysis. It needs to point out that progress achieved for any friction-based joining process may be helpful to improve the other friction-based joining processes, as they are principally related.

Declaration of Competing Interest

The authors declare that they have no known competing financial interests or personal relationships that could have appeared to influence the work reported in this paper.

Acknowledgments

F. Balle would like ot thank the German Research Foundation (DFG) for the financial support of the work on ultrasonic welding (FOR 524, BA 4073/9-1) as well as several industrial partners (Airbus, CTC) for fruitful discussions and materials support.

S.T. Amancio-Filho gratefully acknowledge his financial support from the Austrian aviation program “TAKE OFF” and from the Austrian Ministry for Climate Action, Environment, Energy, Mobility, Innovation and Technology BMK”.

References

[1] Zhou Y, Fan H, Jiang K, Gou M, Li N, Zhu P, et al. Experimental flexural behaviors of CFRP strengthened aluminum beams. Compos Struct 2014;116:761–71.
[2] Meng F, Li W, Fan H, Zhou Y. A nonlinear theory for CFRP strengthened aluminum beam. Compos Struct 2015;131:574–7.
[3] Zhao X-L, Zhang L. State-of-the-art review on FRP strengthened steel structures. Eng Struct 2007;29:1808–23.
[4] Teng JG, Yu T, Fernando D. Strengthening of steel structures with fiber-reinforced polymer composites. J Constr Steel Res 2012;78:131–43.
[5] Harries KA, Peck AJ, Abraham EJ. Enhancing stability of structural steel sections using FRP. Thin-Walled Struct 2009;47:1092–101.
[6] Christke S, Gibson AG, Grigoriou K, Mouritz AP. Multi-layer polymer metal laminates for the fire protection of lightweight structures. Mater Des 2016;97:349–56.
[7] Lambiase F, Durante M. Mechanical behavior of punched holes produced on thin glass fiber reinforced plastic laminates. Compos Struct 2017;173:25–34.
[8] Borba NZ, de Macêdo SCM, dos Santos JF, Canto LB, Amancio-Filho ST. Direct-friction riveting of metal-cfrp overlap joints. ANTEC Paper Society of Plastics Engineers, Orlando, FA, USA, 2018.
[9] Lambiase F, Paoletti A, Di Ilio A. Advances in mechanical clinching: employment of a rotating tool. In: Procedia Engineering. p. 200–5.
[10] Lambiase F, Paoletti A. Friction-assisted clinching of Aluminum and CFRP sheets. J Manuf Processes 2018;31:812–22.
[11] Katayama S. Handbook of laser welding technologies. Woodhead Publishing; 2013.
[12] Di Franco G, Fratini L, Pasta A. Influence of the distance between rivets in self-piercing riveting bonded joints made of carbon fiber panels and AA2024 blanks. Mater Des 2012;35:342–9.
[13] Franco G, Fratini L, Pasta A, Ruisi AF. On the self-piercing riveting of aluminium blanks and carbon fibre composite panels. Int J Mater Form 2010;3:1035–8.
[14] Meschut G, Gude M, Augenthaler F, Geske V. Evaluation of damage to carbon-fibre composites induced by self-pierce riveting. Procedia CIRP 2014;18:186–91.
[15] Mandel M, Krüger L. Electrochemical corrosion studies and pitting corrosion sensitivity of a self-pierce rivet joint of carbon fibre reinforced polymer (CFRP) – laminate and EN AW-6060-T6. Material wissenschaft und Werkstofftechnik 2012;43:302–9.
[16] Yeh R-Y, Hsu R-Q. Development of ultrasonic direct joining of thermoplastic to laser structured metal. Int J Adhes Adhes 2016;65:28–32.
[17] Lionetto F, Balle F, Maffezzoli A. Hybrid ultrasonic spot welding of aluminum to carbon fiber reinforced epoxy composites. J Mater Process Technol 2017;247:289–95.
[18] Lionetto F, Mele C, Leo P, D'Ostuni S, Balle F, Maffezzoli A. Ultrasonic spot welding of carbon fiber reinforced epoxy composites to aluminum: mechanical and electrochemical characterization. Compos B Eng 2018;144:134–42.
[19] Krüger S, Wagner G, Eifler D. Ultrasonic welding of metal/composite joints. Adv Eng Mater 2004;6:157–9.
[20] Balle F, Eifler D. Statistical test planning for ultrasonic welding of dissimilar materials using the example of aluminum-carbon fiber reinforced polymers (CFRP) joints. Materialwiss Werkstofftech 2012;43:286–92.
[21] Wagner G, Balle F, Eifler D. Ultrasonic welding of aluminum alloys to fiber reinforced polymers. Adv Eng Mater 2013;15:792–803.
[22] Balle F, Huxhold S, Emrich S, Wagner G, Kopnarski M, Eifler D. Influence of heat treatments on the mechanical properties of ultrasonic welded AA 2024/CF-PA66-joints. Adv Eng Mater 2013;15:837–45.
[23] Magin J, Balle F. Solid state joining of aluminum, titanium and their hybrids by ultrasonic torsion welding. Materialwiss Werkstofftech 2014;45:1072–83.
[24] Staab F, Balle F. Ultrasonic torsion welding of ageing-resistant Al/CFRP joints: properties, microstructure and joint formation. Ultrasonics 2019;93:139–44.
[25] Feistauer EE, Guimarães RPM, Ebel T, dos Santos JF, Amancio-Filho ST. Ultrasonic joining: A novel direct-assembly technique for metal-composite hybrid structures. Mater Lett 2016;170:1–4.
[26] Feistauer EE, Ebel T, dos Santos JF, Amancio-Filho ST. Amancio-Filho, Ultrasonic joining of through-the-thickness reinforced Ti-4Al-6V and polyetherimide hybrid joints. In: ANTEC, Society of Plastics Engineers, Anaheim, CA, USA. p. 1718–24.
[27] Feistauer EE, Amancio-Filho ST. Ultrasonic joining of lightweight alloy/fiber-reinforced polymer hybrid structures. In: Blaga STA-FAL-A, editor. Joining of Polymer-Metal Hybrid Structures: Principles and Applications. USA: Wiley; 2018. p. 249–74.
[28] Feistauer EE, dos Santos JF, Amancio-Filho ST. An investigation of the ultrasonic joining process parameters effect on the mechanical properties of metal-composite hybrid joints. Weld World 2020;64:1481–95.
[29] Junior WS, Handge UA, dos Santos JF, Abetz V, Amancio-Filho ST. Feasibility study of friction spot welding of dissimilar single-lap joint between poly(methyl methacrylate) and poly(methyl methacrylate)-SiO2 nanocomposite. Mater Des 2014;64:246–50.
[30] Goushegir SM, dos Santos JF, Amancio-Filho ST. Friction Spot Joining of aluminum AA2024/carbon-fiber reinforced poly(phenylene sulfide) composite single lap joints: microstructure and mechanical performance. Mater Des 2014;54:196–206.
[31] Esteves JV, Goushegir SM, dos Santos JF, Canto LB, Hage E, Amancio-Filho ST. Friction spot joining of aluminum AA6181-T4 and carbon fiber-reinforced poly (phenylene sulfide): effects of process parameters on the microstructure and mechanical strength. Mater Des 2015;66:437–45.
[32] Goushegir SM, dos Santos JF, Amancio-Filho ST. Influence of process parameters on mechanical performance and bonding area of AA2024/carbon-fiber-reinforced poly(phenylene sulfide) friction spot single lap joints. Mater Des 2015;83:431–42.
[33] Amancio-Filho ST, Bueno C, dos Santos JF, Huber N, Hage E. On the feasibility of friction spot joining in magnesium/fiber-reinforced polymer composite hybrid structures. Mater Sci Eng, A 2011;528:3841–8.

[34] Yusof F, Miyashita Y, Seo N, Mutoh Y, Moshwan R. Utilising friction spot joining for dissimilar joint between aluminium alloy (A5052) and polyethylene terephthalate. Sci Technol Weld Join 2013;17:544–9.
[35] Huang Y, Meng X, Xie Y, Lv Z, Wan L, Cao J, et al. Friction spot welding of carbon fiber-reinforced polyetherimide laminate. Compos Struct 2018;189:627–34.
[36] Lambiase F, Genna S, Kant R. A procedure for calibration and validation of FE modelling of laser-assisted metal to polymer direct joining. Opt Laser Technol 2018;98:363–72.
[37] Lambiase F, Genna S. Laser assisted joining of AA5053 aluminum alloy with polyvinyl chloride (PVC). Opt Laser Technol 2018;107:80–8.
[38] Chen YJ, Yue TM, Guo ZN. Laser joining of metals to plastics with ultrasonic vibration. J Mater Process Technol 2017;249:441–51.
[39] Zhang Z, Shan J-G, Tan X-H, Zhang J. Effect of anodizing pretreatment on laser joining CFRP to aluminum alloy A6061. Int J Adhes Adhes 2016;70:142–51.
[40] Tamrin KF, Nukman Y, Zakariyah SS. Laser lap joining of dissimilar materials – a review of factors affecting joint strength 130715070734009. Mater Manuf Processes 2013.
[41] Huang Y, Meng X, Xie Y, Li J, Si X, Fan Q. Improving mechanical properties of composite/metal friction stir lap welding joints via a taper-screwed pin with triple facets. J Mater Process Technol 2019;268:80–6.
[42] Huang Y, Meng X, Xie Y, Li J, Wan L. Joining of carbon fiber reinforced thermoplastic and metal via friction stir welding with co-controlling shape and performance. Compos A Appl Sci Manuf 2018;112:328–36.
[43] Huang Y, Meng X, Wang Y, Xie Y, Zhou L. Joining of aluminum alloy and polymer via friction stir lap welding. J Mater Process Technol 2018;257:148–54.
[44] Meng X, Huang Y, Cao J, Shen J, dos Santos JF. Recent progress on control strategies for inherent issues in friction stir welding. Prog Mater Sci 2021;115:100706.
[45] Li X, Xu D, Gong N, Xu Z, Wang L, Dong W. Improving the strength of injection molded aluminum/polyphenylene sulfide lap joints dependence on surface microstructure and composition. Mater Des 2019;179:107875.
[46] Li X, Liu F, Gong N, Yang C, Wang B. Surface topography induced high injection joining strength of polymer-metal composite and fracture mechanism. Compos Struct 2018;184:545–53.
[47] Blaga L, Bancilă R, dos Santos JF, Amancio-Filho ST. Friction Riveting of glass–fibre-reinforced polyetherimide composite and titanium grade 2 hybrid joints. Mater Des 2013;50:825–9.
[48] Altmeyer J, dos Santos JF, Amancio-Filho ST. Effect of the friction riveting process parameters on the joint formation and performance of Ti alloy/short-fibre reinforced polyether ether ketone joints. Mater Des 2014;60:164–76.
[49] Meng X, Huang Y, Xie Y, Li J, Guan M, Wan L, et al. Friction self-riveting welding between polymer matrix composites and metals. Compos A Appl Sci Manuf 2019;127:105624.
[50] Liu FC, Dong P, Lu W, Sun K. On formation of Al O C bonds at aluminum/polyamide joint interface. Appl Surf Sci 2019;466:202–9.
[51] Yusof F, Muhamad M, Moshwan R, Jamaludin M, Miyashita Y. Effect of surface states on joining mechanisms and mechanical properties of aluminum alloy (a5052) and polyethylene terephthalate (PET) by dissimilar friction spot welding. Metals 2016;6:101.
[52] Lambiase F, Paoletti A, Grossi V, Genna S. Improving energy efficiency in friction assisted joining of metals and polymers. J Mater Process Technol 2017;250:379–89.
[53] Lambiase F, Paoletti A, Grossi V, Di Ilio A. Friction assisted joining of aluminum and PVC sheets. J Manuf Process 2017;29:221–31.
[54] Lambiase F, Paoletti A. Friction Assisted Joining of titanium and polyetheretherketone (PEEK) sheets. Thin-Walled Struct 2018;130:254–61.
[55] Lambiase F, Paoletti A. Mechanical behavior of AA5053/polyetheretherketone (PEEK) made by Friction Assisted Joining. Compos Struct 2018;189:70–8.
[56] Lambiase F, Grossi V, Paoletti A. Defects formation during Friction Assisted Joining of metals and semi crystalline polymers. J Manuf Processes 2021;62:833–44.
[57] Lambiase F, Paoletti A, Durante M. Mechanism of bonding of AA7075 aluminum alloy and CFRP during Friction Assisted Joining. Compos Struct 2021;113593.
[58] Liu FC, Liao J, Nakata K. Joining of metal to plastic using friction lap welding. Mater Des 2014;54:236–44.
[59] Liu FC, Liao J, Gao Y, Nakata K. Effect of plasma electrolytic oxidation coating on joining metal to plastic. Sci Technol Weld Joi 2015;20:291–6.
[60] Liu FC, Nakata K, Liao J, Hirota S, Fukui H. Reducing bubbles in friction lap welded joint of magnesium alloy and polyamide. Sci Technol Weld Join 2014;19:578–87.
[61] Kimiaki N, Hironobu T, Bolyu X, Atsuki T, Kazuhiro N. Effect of silane coupling on the joint characteristics of friction lap joined Al alloy/CFRP. Weld Int 2018;32:328–37.
[62] Wu LH, Nagatsuka K, Nakata K. Direct joining of oxygen-free copper and carbon-fiber-reinforced plastic by friction lap joining. J Mater Sci Technol 2018;34:192–7.
[63] Nagatsuka K, Kitagawa D, Yamaoka H, Nakata K. Friction lap joining of thermoplastic materials to carbon steel. ISIJ Int 2016;56:1226–31.
[64] Meyer SP, Wunderling C, Zaeh MF. Influence of the laser-based surface modification on the bond strength for friction press joining of aluminum and polyethylene. Prod Eng Res Devel 2019:1–10.
[65] Nagatsuka K, Yoshida S, Tsuchiya A, Nakata K. Direct joining of carbon-fiber-reinforced plastic to an aluminum alloy using friction lap joining. Compos Part B-Eng 2015;73:82–8.
[66] Liu F, Dong P. Promising high-speed welding techniques for joining polymers to metals and underlying joining mechanisms. In: Friction Stir Welding and Processing X. Springer; 2019. p. 13–22.
[67] Liu FC, Dong P, Pei X. A high-speed metal-to-polymer direct joining technique and underlying bonding mechanisms. J Mater Process Technol 2020;280:116610.
[68] Amancio-Filho ST, Blaga L-A. Joining of polymer-metal hybrid structures: principles and applications; 2018.
[69] Borba NZ, Blaga L, dos Santos JF, Amancio-Filho ST. Direct-Friction Riveting of polymer composite laminates for aircraft applications. Mater Lett 2018;215:31–4.
[70] Amancio-Filho ST, Beyer M, dos Santos JF. Method of connecting a metallic bolt to a plastic workpiece. in 2009.
[71] Gagliardi F, Conte R, Ciancio C, Simeoli G, Pagliarulo V, Ambrogio G, et al. Joining of thermoplastic structures by Friction Riveting: a mechanical and a microstructural investigation on pure and glass reinforced polyamide sheets. Compos Struct 2018;204:268–75.
[72] Hynes NRJ, Vignesh NJ, Velu PS. Low-speed friction riveting: a new method for joining polymer/metal hybrid structures for aerospace applications. J Braz Soc Mech Sci Eng 2020;42.
[73] Amancio-Filho ST. Friction Riveting: development and analysis of a new joining technique for polymer-metal multi-material structures. Weld World 2011:13–24.
[74] Amancio-Filho ST, dos Santos JF. Preliminary analytical modelling of heat input in friction riveting. In: ANTEC Society of Plastics Engineers Indianapolis, Indiana, USA; 2016 p. 1310–7.
[75] Pina Cipriano G, Ahiya A, dos Santos JF, Vilaça P, Amancio-Filho ST. Single-phase friction riveting: metallic rivet deformation, temperature evolution, and joint mechanical performance. Weld World 2019;64:47–58.
[76] Bock FE, Blaga LA, Klusemann B. Mechanical performance prediction for friction riveting joints of dissimilar materials via machine learning. Procedia Manuf 2020;47:615–22.
[77] Borba NZ, Kötter B, Fiedler B, dos Santos JF, Amancio-Filho ST. Mechanical integrity of friction-riveted joints for aircraft applications. Compos Struct 2020;232:111542.
[78] Cipriano LABGP, dos Santos JF, Vilaça P, Amancio-Filho ST. Fundamentals of force-controlled friction riveting: Part II-Joint global mechanical performance and energy efficiency. Materials (Basel) 2018;11:2489.
[79] Amancio-Filho ST, dos Santos, European Patent 2329905B1; 2012.
[80] Schilling C, dos Santos JF. International Patent WO/2001/036144; 2005.
[81] Amancio-Filho ST, Camillo APC, Bergmann L, Santos JFD, Kury S, Atilde EO, et al. Preliminary Investigation of the Microstructure and Mechanical Behaviour of 2024 Aluminium Alloy Friction Spot Welds. Mater. Trans. 2011;52:985–91.
[82] Gonçalves J, dos Santos JF, Canto LB, Amancio-Filho ST. Friction spot welding of carbon fiber-reinforced polyamide 66 laminate. Mater Lett 2015;159:506–9.
[83] André NM. Mechanical integrity and corrosion behavior of metal-composite hybrid joints produced with Friction Spot Joining PhD Thesis, in:. Germany: Hamburg University of Technology (TUHH); 2020.
[84] N. Manente André, F.D.S. J, T.A.-F. S, Evaluation of Joint Formation and Mechanical Performance of the AA7075-T6/CFRP Spot Joints Produced by Frictional Heat, Materials (Basel); 2019. p. 12.
[85] Goushegir SM, dos Santos JF, Amancio-Filho ST. Friction Spot Joining of aluminum AA2024/carbon-fiber reinforced poly(phenylene sulfide) composite single lap joints: Microstructure and mechanical performance. Mater. Des. (1980–2015) 2014;54:196–206.
[86] Goushegir SM, Scharnagl N, dos Santos JF, Amancio-Filho ST. XPS analysis of the interface between AA2024-T3/CF-PPS friction spot joints. Surf Interface Anal 2016;48:706–11.
[87] Junior WS, Amancio-Filho ST, Abetz V, dos Santos JF. European Patent 2993029 B1; 2016.
[88] Goushegir SM, dos Santos JF, Amancio-Filho ST. Failure and fracture micro-mechanisms in metal-composite single lap joints produced by welding-based joining techniques. Compos A Appl Sci Manuf 2016;81:121–8.
[89] Goushegir SM. Friction Spot Joining of Metal-Composite Hybrid Structures PhD thesis. Hamburg, Germany: Hamburg University of Technology (TUHH); 2015.
[90] Staab F, Liesegang M, Balle F. Local shear strength distribution of ultrasonically welded hybrid Aluminium to CFRP joints. Compos Struct 2020;248:112481.
[91] Lambiase F, Di Ilio A, Paoletti A. Hybrid numerical modeling of Friction Assisted Joining. J Manuf Processes 2020;57:233–43.
[92] Lambiase F, Paoletti A, Di Ilio A. Forces and temperature variation during friction stir welding of aluminum alloy AA6082-T6. Int J Adv Manuf Technol 2018;99:337–46.
[93] Lambiase F, Grossi V, Paoletti A. Machine learning applied for process design of hybrid metal-polymer joints. J Manuf Processes 2020;58:92–100.
[94] Goushegir SM, dos Santos JF, Amancio-Filho ST. Influence of aluminum surface pre-treatments on the bonding mechanisms and mechanical performance of metal-composite single-lap joints. Weld World 2017;61:1099–115.
[95] André NM, Goushegir SM, dos Santos JF, Canto LB, Amancio-Filho ST. Friction Spot Joining of aluminum alloy 2024–T3 and carbon-fiber-reinforced poly (phenylene sulfide) laminate with additional PPS film interlayer: Microstructure, mechanical strength and failure mechanisms. Compos B Eng 2016;94:197–208.
[96] André NM, Goushegir SM, Santos JFd, Canto LB, Amancio-Filho ST. Influência da Espessura do Filme Polimérico Intermediário na Resistência Mecânica de Juntas Híbridas de Alumínio 2024-T3 e CF-PPS Produzidas por União Pontual por Fricção. Soldagem & Inspeção 2016;21:2–15.
[97] Manente André N, Goushegir SM, Scharnagl N, dos Santos JF, Canto LB, Amancio-Filho ST. Composite surface pre-treatments: improvement on adhesion mechanisms and mechanical performance of metal–composite friction spot joints with additional film interlayer. J Adhes 2018;94:723–42.

[98] Ebnesajjad S. Surface treatment of materials for adhesive bonding. 2nd ed. Oxford: W.A. Publishing; 2014. p. 77–91.
[99] André NM, dos Santos JF, Amancio-Filho ST. Impact resistance of metal-composite hybrid joints produced by frictional heat. Compos Struct 2020;233:111754.
[100] Goushegir SM, Scharnagl N, Dos Santos JF, Amancio-Filho ST. Durability of metal-composite friction spot joints under environmental conditions. Materials (Basel) 2020;13.
[101] André NM, Bouali A, Maawad E, Staron P, Santos JFd, Zheludkevich ML, et al. Corrosion behavior of metal–composite hybrid joints: influence of precipitation state and bonding zones. Corros Sci 2019;158. 108075.
[102] Borba NZ. Design and mechanical integrity of friction riveted joints of thermoplastic composite PhD Thesis. Germany: Hamburg University of Technology (TUHH); 2020.
[103] Schmeer S, Balle F, Didi M, Wagner G, Maier M, Mitschang P. Experimental and numerical characterization of spot welded hybrid Al/CFRP-joints on coupon level. Adv Eng Mater 2013;15:853–60.